

Phase Memory in Electron Spin Echoes, Lattice Relaxation Effects in $\text{CaWO}_4:\text{Er}$, Ce , Mn

W. B. MIMS*

Bell Telephone Laboratories, Murray Hill, New Jersey

(Received 4 October 1967)

The electron-spin-echo phase memory T_M has been studied both experimentally and theoretically for the specific case in which it is limited by the lattice relaxation processes occurring in the sample. The relevant mechanism is as follows. Lattice relaxation of any spins, whether or not they belong to the species being observed, causes fluctuations in the local fields and so destroys the relations between precessional phases which lead to the generation of echoes. The effect of these fluctuations on the echo amplitude can be calculated by taking an ensemble average for the precessing spins and for all the environmental spins which give rise to significant time variations of the local fields in the sample. The problem reduces to that of finding a time and a space average. The space average has been obtained here by assuming a random distribution of spins in the paramagnetic sample, and by applying the statistical methods of Margenau. In order to obtain the time average, two models have been chosen to represent the time variation of the components μ_z for the relaxing spins. In one model, the μ_z are treated as Gaussian random variables (Gauss-Markoff model), and in the other the spins are assumed to make sudden jumps at random times between the "spin-up" and "spin-down" quantum states (sudden-jump model). Different forms of echo envelope are derived for the two models. Further differences in behavior will be observed, according to whether the sample is singly or doubly doped. If the sample contains only one spin species, T_M becomes shorter as the temperature is raised and as the lattice relaxation time T_1 is reduced. Initially, T_M is limited by local field fluctuations and may be considerably shorter than T_1 . Eventually, as the lattice relaxation of the precessing spins themselves becomes the dominant factor, T_1 and T_M tend to the same value. If the sample contains two species A and B , where B relaxes more rapidly than A , then $T_M(A)$ and $T_M(B)$ both begin by shortening as $T_1(B)$ is reduced. For very small values of $T_1(B)$, however, $T_M(A)$ lengthens again. The rapidly fluctuating local fields due to the B -spins produce a diminishing effect on the A spins, the phenomenon being analogous to motional narrowing. The form of the A -spin echo envelope in the limit of rapid B -spin relaxation does not depend on the model chosen to represent the time variation of μ_z during the relaxation of the B spins.

Experimental results are presented for two-pulse and three-pulse echoes, and are compared with the calculations. The material is CaWO_4 doped with Ce and Er or with Mn and Er . At the lower temperatures, the results are in moderately good agreement with the Gauss-Markoff theory. At higher temperatures, the results can only be explained by assuming that the transition rate between the levels of the Er ground doublet is an order of magnitude higher than the transition rate inferred from T_1 measurements. It is tentatively suggested that this may arise from the fact that T_M depends on the arithmetic sum of the upward and downward transitions, whereas T_1 merely measures the algebraic sum, i.e., the excess of downward over upward transitions. If some form of spin-spin interaction is taking place, or if there is a phonon bottleneck (or any other mechanism causing transfers of energy within the spin system), the absolute and the net transition rates will cease to bear the usual thermodynamic relation to one another. In the present case it is suggested that energy transfer in the Er spin system is accelerated by the exchange of real phonons as soon as there is a significant population of the first excited doublet. The possible effects of spin clustering and of nonmagnetic dipolar interactions on the form of the echo decay envelopes are also briefly discussed.

I. INTRODUCTION

IN this paper we present calculations and experimental measurements of the decay function or echo envelope for two-pulse echoes when decay is controlled by lattice relaxation processes.^{1,2} The echo phase memory time, T_M , cannot exceed the lattice relaxation time T_1 of the spin species which is being observed. Echo phase memories can, however, often be considerably shorter than T_1 even in a regime where they are varying rapidly with temperature and are thus clearly dependent on lattice relaxation effects. They are, moreover, sensitive to the lattice relaxation of other spin

species present in the sample, the phase memory of any resonance line being a function of the behavior of the total paramagnetic environment in the host material. The effect of the paramagnetic environment can be understood as follows. Let us divide the spins in the sample into two groups: a group A which has been prepared for echo generation by the application of microwave pulses and a group B which consists of the remaining spins.³ Groups A and B interact via the $S_z(A)S_z(B)$ term in the dipolar Hamiltonian. If group B relaxes to the lattice, the effect is to generate a fluctuating local field acting on group A which causes the Larmor frequencies to undergo small shifts and the precessional phases to be randomized. This mechanism may be operative even if there is only one spin species present. Suppose, for example, that a fraction

* Present address: Department of Physics, University of California, Los Angeles, Calif. 90024.

¹ This problem has been discussed previously in a theoretical paper by J. R. Klauder and P. W. Anderson, *Phys. Rev.* **125**, 912 (1962).

² Earlier experimental results are given by W. B. Mims, K. Nassau, and J. D. McGee, *Phys. Rev.* **123**, 2059 (1961).

³ A discussion in terms of A - and B -spin groups of some analogous problems in NMR is given by B. Herzog and E. L. Hahn, *Phys. Rev.* **103**, 148 (1956).

of the spins which have been prepared by the microwave pulses relax to the lattice before the echo signal appears. These spins are, of course, lost to the A -spin group and do not contribute to the signal. There is thus a certain degree of A -spin attenuation. If, however, the relaxation of these spins causes an appreciable change in the local field configurations in the sample, then, the same spins, acting as B spins, will cause some additional attenuation of the echo signal. In many cases this B -spin effect is larger than the A -spin attenuation.

When the A - and B -spin groups belong to the same resonance line, the phase memory becomes shorter as T_1 is reduced and as the local field fluctuations become more rapid. Eventually a point is reached when direct lattice relaxation of the precessing spins (i.e., the A -spin effect) becomes more important than the local field effects (the B -spin effect) and the echo envelope follows the lattice relaxation curve. If the B spins belong to a different, and more rapidly relaxing species a new feature may appear. As $T_1(B)$ is reduced, the A -spin phase memory will first shorten and then lengthen out again. This is an effect analogous to exchange or motional narrowing⁴ and is due to the rapid averaging of the local field fluctuations. Altogether the phase memory of the A -spin group in such a doubly doped sample will show the following changes as the lattice temperature T_L is increased:

- (a) The phase memory will shorten because of local field "noise" generated by B -spin relaxation.
- (b) There will be a subsequent lengthening as B -spin relaxation becomes too rapid to have any effect.
- (c) The phase memory will fall once more as the A spins themselves take over the role of B spins until finally T_M and $T_1(A)$ tend to the same value.

In practice it is quite difficult to study ranges (a), (b), (c) in isolation from each other, and to eliminate the effects of other processes such as spin-spin flips which also create local field noise. Spin-spin flips can occur within the A - or B -spin groups or amongst the nuclei in the host lattice, and the analysis of their effects poses a difficult theoretical problem which is not treated here. As far as possible, these complications have been minimized in the present experimental studies by choosing suitable samples, and by selecting experimental conditions under which a particular mechanism predominates. Phase-memory times have been measured in the three ranges and echo-envelope-decay curves have been obtained which illustrate the two different types of behavior found in ranges (a) or (c) and in range (b).

The phase-memory time T_M in a two-pulse spin echo experiment is here defined as the time between *pulse I* and *the echo* which must elapse to bring about an e^{-1}

attenuation of the echo signal.⁵ T_M conveys only a limited amount of information, since the echo is not, in general, exponential and does not always have the same mathematical form, but it is useful as a rough measure of the time scale of the decay. An echo envelope of nonexponential form cannot, of course, be properly described by a relaxation time T_2 . Nevertheless it may sometimes be convenient to treat T_M and T_2 as equivalent in rough calculations. It should also be stressed that, even when T_M is controlled by flip-flop processes, it does not normally give a direct measure of the flip-flop transition time. Control of T_M by flip-flop transitions is, like control of T_M by lattice relaxation processes, usually an environmental or B spin rather than a direct or A -spin effect.

Interactions between A spins and B spins can lead to echo attenuation in three-pulse as well as in two-pulse experiments. In a three-pulse, or stimulated echo experiment the echo signal attenuation depends on the times τ and T which elapse between pulses I and II and between pulses II and III, respectively. When $T_1(B) \gg T$ the decay during time T is interpreted in terms of a spectral diffusion process which arises from changes in the local fields. The same basic considerations apply as in the case of the two-pulse phase memory, so that the assumptions of the models which we discuss here can be tested by performing either type of experiment. This is no longer true, however, when $T_1(B)$ is short. Local fields are then averaged and the concept of spectral diffusion has no useful meaning.

Theoretical calculations are given in Secs. II and III and in the Appendices. Experimental results are presented in Sec. IV and are discussed in Sec. V.

II. TWO-PULSE ECHOES—THEORY

We begin by showing how the envelope decay function can be factored out of the general expression for spin echoes, and indicate the conditions which must be satisfied if this function is to be independent of the linewidth and of the pulse power. Let us first consider the generation of echoes by A spins in the absence of B spins. Dipolar interactions between A spins are ignored, and, in the event of the A spins having a multi-level system, we select only those two levels which are involved in the resonance. The state of the system of N A spins after the first applied microwave pulse can be described by a $2N \times 2N$ density matrix consisting of $N \times 2 \times 2$ submatrices of the form

$$\begin{bmatrix} \rho_{11} & a_I e^{i\omega t} \\ a_I^* e^{-i\omega t} & \rho_{22} \end{bmatrix} \quad (1)$$

arranged along the diagonal. $\hbar\omega$ is the energy difference between the two states and a_I depends on the inter-

⁴ A. Abragam, *The Principles of Nuclear Magnetism* (Oxford University Press, New York, 1961). See also Ref. 9.

⁵ The word "signal" is used as an abbreviation for "precessing magnetization." The voltage output signal obtained from a superheterodyne receiver is essentially proportional to the precessing magnetization in the sample.

action with the microwave field during the pulse. When the second microwave pulse is applied at time τ , each 2×2 submatrix is changed to

$$\begin{bmatrix} \rho_{II}' & a_{I'}^* a_{II} e^{-i\omega\tau} e^{i\omega(t-\tau)} + b_{II} e^{i\omega(t-\tau)} \\ a_{II} a_{I'}^* e^{i\omega\tau} e^{-i\omega(t-\tau)} + b_{II}^* e^{-i\omega(t-\tau)} & \rho_{22}' \end{bmatrix}, \quad (2)$$

where a_{II} depends on the interaction with the second pulse. The echo signal is found by calculating $\text{Tr}(\rho M_x)$ and arises from the terms with coefficients $a_{I'}^* a_{II}$. Assuming that the number of systems having an energy separation $\hbar\omega$ can be specified by means of a distribution $g(\omega)$ we have that

$$\text{Tr}(\rho M_x) \propto \text{Re} \left(\int g(\omega) a_{I'}^*(\omega) a_{II}(\omega) e^{i\omega(t-2\tau)} d\omega \right). \quad (3)$$

The echo signal is generated at $t = 2\tau$ and its form is given by the Fourier cosine transform of $g(\omega) a_{I'}^*(\omega) a_{II}(\omega)$. The functions $a_{I'}(\omega)$, $a_{II}(\omega)$, which must be calculated by considering in detail the motion of a spin in the applied microwave field H_1 for a given ω , are generally somewhat involved and the echo signal can assume a variety of complicated forms.⁷ A picture which is approximately correct under normal pulsing conditions can, however, be obtained by taking $a_{I'}$ and a_{II} to be Lorentzian functions with a half-width at half-height of γH_1 . In NMR work it is often possible to make the further assumption that γH_1 is several times greater than the width of $g(\omega)$. The factors $a_{I'}(\omega)$ and $a_{II}(\omega)$ then vary slowly over the range of interest and can be taken outside the integral in Eq. (3), leaving the echo waveform as the Fourier transform of $g(\omega)$. This very simple situation cannot always be reproduced in ESR work, where strains and other inhomogeneous broadening mechanisms sometimes result in wide resonance lines. At practicable microwave power levels $g(\omega)$ is often wider than γH_1 , causing the form of the echo signal to depend primarily on the pulsing conditions via the factors $a_{I'}$ and a_{II} in Eq. (3). In general, however, the echo waveform does not vary as τ is increased. Also, as is shown in the next paragraph, the measurement of decay times is not affected by the pulsing conditions, provided that changes in the *B*-spin local fields during a time 2τ are less than γH_1 .

The lattice relaxation of the *B* spins and their interaction with the *A* spins might be introduced into the problem by expanding the density matrix so as to include the *B* spins and the lattice modes. A rigorous solution would then be obtained by following the evolution of $\text{Tr}(\rho M_x)$ at time 2τ as a function of τ . The

enormous complication inherent in such an approach can however be largely avoided by adopting a physical model as outlined in the Introduction. We suppose that the interaction with *B* spins changes the frequencies ω by an amount

$$\Delta\omega(t) = \gamma_A \sum_j \mu_j(t) (1 - 3 \cos^2 \theta_j) / r_j^3, \quad (4)$$

where $\mu_j(t)$ is the time-varying component of magnetization parallel to the Zeeman field H_0 of the *j*th *B* spin, i.e., the matrix element of $g_B \beta S_z^j(t)$. The other quantities in (4) are defined in Appendix A. Since, under the action of *B*-spin local fields, the *A* spins no longer preserve their frequencies ω , the exponents $\omega\tau$, $\omega(t-\tau)$ in the off-diagonal term in (2) must be replaced by integrals. The $a_{I'}^* a_{II}$ term becomes

$$a_{I'}^*(\omega_0) a_{II}(\omega_\tau) \exp \left\{ i \int_0^{2\tau} s(t') \omega(t') dt' \right\},$$

where ω_0 , ω_τ are the values of ω at times $t=0$, $t=\tau$, and where $s(t')$ is the function introduced by Klauder and Anderson⁸ to take into account the phase reversal occurring at time τ . $s(t)$ has the value $+1$ when $t < \tau$ and -1 when $t > \tau$. Equation (3) now becomes

$$\text{Tr}(\rho M_x) \propto \text{Re} \left(\int g(\omega_0) a_{I'}^*(\omega_0) a_{II}(\omega_\tau) \times \exp \left\{ i \int s(t') \omega(t') dt' \right\} d\omega_0 \right). \quad (5)$$

The summation (or average) over *A* spins denoted by the first integral can be simplified if we assume that $a_{I'}$ and a_{II} vary only slightly over the interval $\omega_\tau - \omega_0$. Under normal pulsing conditions this requires that $\omega_\tau - \omega_0 < \gamma H_1$. We can then write $a_{II}(\omega_\tau) \simeq a_{II}(\omega_0)$, and the integral (5) may then be factored to give

$$\text{Tr}(\rho M_x) \propto \text{Re} \left(\int g(\omega_0) a_{I'}^*(\omega_0) a_{II}(\omega_0) e^{i\omega_0(t-2\tau)} d\omega_0 \right) \times \exp \left\{ i \int_0^{2\tau} s(t') (\Delta\omega(t') - \Delta\omega(0)) dt' \right\}_{AV}. \quad (6)$$

The first factor in (6) is then the same as the integral (3), and the echo signal is a product of the two factors, a waveform factor depending on $g(\omega)$ and on the pulsing conditions, and a "phase-memory" factor depending

⁶ For simplicity it is assumed here that $\tau \gg t_p$, where t_p is the duration of the applied pulses. Detailed calculations show that the peak of the observed signal may move by $\sim \frac{1}{2} t_p$ according to the pulsing conditions (see also Ref. 7).

⁷ The motion of spins in applied rf fields has been analyzed by A. L. Bloom, Phys. Rev. **98**, 1105 (1955). Some numerical computations of echo waveforms have been made by W. B. Mims, Rev. Sci. Instr. **36**, 1472 (1965).

⁸ See Ref. 1, Eq. (1.8).

on an average calculated from the individual frequency changes, $\Delta\omega(t)$, due to the local fields.

Substituting (4) in the second factor of (6) we obtain the phase memory factor, or echo decay function

$$E(2\tau) = \left\langle \left\langle \exp i \left\{ \int_0^{2\tau} [s(t') \gamma_A \sum_j (\mu_j(t') - \mu_j(0)) \times (1 - 3 \cos^2 \theta_j) / r_j^3] dt' \right\} \right\rangle_{Av \text{ i}} \right\rangle_{Av \text{ ii}}. \quad (7)$$

The meaning of the double average is as follows. Average i is taken over a subensemble of A spins, all of them having B spins at a particular set of related lattice points. Average ii is over all possible types of spin neighborhoods. Average i can be replaced by a time average according to the ergodic hypothesis, whereas average ii is over a set of permanent configurations established at the time when the crystal was grown and annealed. Writing

$$\xi_j(t) = \int_0^t dt' s(t') (\mu_j(t') - \mu_j(0)) \quad (8a)$$

and

$$\alpha_j = \gamma_A (1 - 3 \cos^2 \theta_j) / r_j^3, \quad (8b)$$

we have

$$E(2\tau) = \left\langle \left\langle \exp i \left\{ \sum_j \alpha_j \xi_j(2\tau) \right\} \right\rangle_{\text{time } Av} \right\rangle_{\text{lattice } Av}, \quad (8c)$$

the lattice average being understood in the sense of average ii.

The first problem is that of finding the time average. This may be done by making two further assumptions which, following Anderson,⁹ we may describe as the Gauss-Markoff model. Let $\mu_j(t)$ be a Gaussian random function. Then $\xi_j(t)$, being a linear combination of the

values of a Gaussian random function is itself randomly distributed with a Gaussian probability curve, and the time mean from (8c) is given by

$$\exp(i\alpha_j \langle \xi_j(2\tau) \rangle) \exp\{-0.5\alpha_j^2 \langle (\xi_j(2\tau))^2 \rangle\}.$$

$\langle \xi_j(2\tau) \rangle$ is the mean and $\langle (\xi_j(2\tau))^2 \rangle$ the variance $\langle (\xi_j(2\tau) - \langle \xi_j(2\tau) \rangle)^2 \rangle$ of $\xi_j(2\tau)$. If we assume that $\langle \mu_j(0) \rangle = 0$, then

$$\langle \xi_j(2\tau) \rangle = \int_0^{2\tau} dt' s(t') \langle \mu_j(t') \rangle.$$

The phase reversal implicit in $s(t')$ will, furthermore, ensure that $\langle \xi_j(2\tau) \rangle = 0$. From (8) we have therefore

$$E(2\tau) = \langle \exp\{-0.5 \sum_j \alpha_j^2 \langle (\xi_j(2\tau))^2 \rangle\} \rangle_{\text{lattice } Av}, \quad (9)$$

where

$$\langle (\xi_j(2\tau))^2 \rangle = \int_0^{2\tau} dt' \int_0^{2\tau} dt'' s(t') s(t'') \times \langle \mu_j(t') \mu_j(t'') \rangle_{\text{time } Av}. \quad (10)$$

To evaluate (10) we introduce the Markoffian assumption

$$\langle \mu_j(t') \mu_j(t'') \rangle = \langle \mu_j(0) \mu_j(t'' - t') \rangle = \langle (\mu_j(0))^2 \rangle \exp\{-R_j |t'' - t'| \}. \quad (11)$$

R_j may be identified with the reciprocal lattice time $1/T_1$ ¹⁰ of the B spins, and $\langle (\mu_j(0))^2 \rangle = \frac{1}{4} g_B^2 \beta^2$. Thus

$$\langle \mu_j(t') \mu_j(t'') \rangle = \frac{1}{4} g_B^2 \beta^2 \exp\{-|t'' - t'| / T_1 \}. \quad (12)$$

Substituting (12) in (10) and performing the integration, we have $\langle (\xi_j(2\tau))^2 \rangle = g_B^2 \beta^2 B(\tau)$, where

$$B(\tau) = (1/R^2) \{ R\tau - (1 - e^{-R\tau}) - 0.5(1 - e^{-R\tau})^2 \}. \quad (13)$$

In terms of $B(\tau)$,

$$E(2\tau) = \langle \exp[-0.5 g_B^2 \beta^2 B(\tau) \sum_j \alpha_j^2] \rangle_{\text{lattice } Av}, \\ = \langle \exp[-0.5 g_B^2 \beta^2 \gamma_A^2 B(\tau) \sum_j (1 - 3 \cos^2 \theta_j)^2 / r_j^6] \rangle_{\text{lattice } Av}. \quad (14)$$

The average over all environments may be found by methods analogous to those used to derive the line-shape function for broadening due to a static B -spin environment (Appendix A).¹¹ Each sum \sum_j contributing to the average corresponds to a particular configuration of B spins about an A spin. Let us suppose that this is arrived at by placing N B spins, one in each of N specified volume elements dV_1, dV_2, \dots, dV_N . If V is the volume of the sample, and if all points are equally likely as sites for the j th B spin, the prob-

ability of finding such a configuration is

$$\prod_j^N (dV_j/V).$$

The contribution to $E(2\tau)$ arising from this configuration is therefore given by

$$\prod_j^N (dV_j/V)$$

⁹ P. W. Anderson, J. Phys. Soc. Japan **9**, 316 (1954). Exchange and motional narrowing problems are treated in this paper.

¹⁰ We use the rate R rather than $1/T_1$ in these calculations in order to simplify the writing out of equations and in order to facilitate comparison with other work (e.g., Ref. 3).

¹¹ The separation of $E(2\tau)$ into a time average and a lattice average as performed here requires the absence of time correlations between the motions of B spins.

multiplied by the exponential inside the brackets in Eq. (14), i.e., it is

$$\left[\prod_j (dV_j/V) \right] \times \exp[-0.5g_B^2\beta^2\gamma_A^2 B(\tau) \sum_j (1-3\cos^2\theta_j)^2/r_j^6]. \quad (15)$$

The average over all possible placements of N B spins in the neighborhood of an A spin is found by integrating over each of the volume elements dV_j . As in the case of the analogous problem in Appendix A this average can be expressed as the product of N similar definite integrals, giving

$$E(2\tau) = \left[(V^{-1}) \int^{v_01} dV \right]^N \times \exp[-0.5B(\tau)g_B^2\beta^2\gamma_A^2(1-3\cos^2\theta)^2/r^6]. \quad (16)$$

By using arguments of the same type as those given in Appendix A we can show that

$$E(2\tau) = [1 - V'/V]^N, \\ = \exp(-n_B V'),$$

where

$$V' = 2\pi \int_0^\infty r^2 dr \int_{-1}^{+1} d(\cos\theta) \\ \times \{1 - \exp[-0.5B(\tau)g_B^2\beta^2\gamma_A^2(1-3\cos^2\theta)^2/r^6]\}. \quad (17)$$

Equation (17) can be integrated to give

$$V' = (8\sqrt{2}\pi I/9\sqrt{3})g_B\beta\gamma_A[B(\tau)]^{1/2}, \quad (18)$$

where I stands for the definite integral

$$\int_0^\infty dx \{1 - \exp(-1/x^2)\}.$$

Substituting the value $I=1.78$ and combining numerical factors we obtain

$$V' = 4.06\gamma_A g_B \beta [B(\tau)]^{1/2}, \quad (19)$$

whence

$$E(2\tau) = \exp\{-4.06n\gamma_A g_B \beta [B(\tau)]^{1/2}\}. \quad (20)$$

Equation (20) can conveniently be reexpressed in terms of the half-width $\Delta\omega_{1/2}$ which would arise from broadening by static B spins [Eq. (A9)]. In these terms

$$E(2\tau) = \exp\{-1.88\Delta\omega_{1/2}[B(\tau)]^{1/2}\} \quad (21)$$

and the required phase-memory function can be obtained by substituting $B(\tau)$ from Eq. (13). The phase-memory time T_M (as defined in the Introduction) is given by twice the root of the equation

$$3.55(\Delta\omega_{1/2})^2 B(\tau) = 1. \quad (22)$$

The result (21) assumes a comparatively simple form in the two limits of $R\tau \ll 1$ and $R\tau \gg 1$. For $R\tau \ll 1$, $B(\tau) = R\tau^3$, and¹²

$$E(2\tau) = \exp\{- (1.88\Delta\omega_{1/2}R^{1/2}\tau^{3/2})\}. \quad (23)$$

At the other limit, when $R\tau \gg 1$, $B(\tau) = \tau/R$ and¹²

$$E(2\tau) = \exp\{- (1.88\Delta\omega_{1/2}R^{-1/2}\tau^{1/2})\}. \quad (24)$$

The two limiting results (23) and (24) can conveniently be expressed in terms of the phase memory in the forms

$$E(2\tau) = \exp\{- (2\tau/T_M)^{3/2}\}, \quad (25a)$$

where

$$T_M = 1.89[R(\Delta\omega_{1/2})^2]^{-1/3}, \quad R\tau \ll 1 \quad (25b)$$

and

$$E(2\tau) = \exp\{- (2\tau/T_M)^{1/2}\}, \quad (26a)$$

where

$$T_M = 0.56R/(\Delta\omega_{1/2})^2, \quad R\tau \gg 1. \quad (26b)$$

The two limiting conditions can also be reformulated in terms of the static local field broadening $\Delta\omega_{1/2}$. Provided that we are only concerned with the first e fall of the echo envelope, the condition $R\tau \ll 1$ is equivalent to $R \ll \Delta\omega_{1/2}$. At the other limit, if $R\tau \gg 1$ holds for the first e fall it will hold for the remainder of the decay, and the condition is equivalent to $R \gg \Delta\omega_{1/2}$. In the intermediate range $R \sim \Delta\omega_{1/2} \sim 1/\tau$, and $E(2\tau)$ cannot be readily approximated by any simpler function. Some calculated decay functions in this range are shown in Fig. 1. The phase memory at the minimum can be found by differentiating (24) with respect to the parameter R contained in $B(\tau)$, giving the results

$$T_M(\min) = 1.8/A\omega_{1/2} \quad (27a)$$

or

$$T_M(\min) = 3.8/R. \quad (27b)$$

The derivation of the decay function $E(2\tau)$ given above depends in a fundamental way on the assumption that $\mu_j(t)$ can be treated as a Gaussian variable. This assumption represents an attempt to summarize the interactions of the B spins and lattice phonons in

¹² In the treatment of analogous problems in NMR expressions of the form $\exp(-cR\tau^3)$ and $\exp(-c'\tau/R)$ are derived for the two limiting cases $R\tau \ll 1$ and $R\tau \gg 1$ (Refs. 3 and 4). The square roots in the exponents of Eqs. (23) and (24) arise as a consequence of the magnetically dilute conditions assumed here. One can understand this difference qualitatively by considering the consequence of random substitution of B spins in the lattice. Some A spins have B spins in their immediate neighborhood and repeatedly undergo large shifts of Larmor frequency; other A spins find themselves in environments where the local fields are always relatively weak. The result is thus approximately equivalent to a superposition of results of the NMR type, but with a distribution of constants c . Equations (23) and (24) are derived by assuming a random placement of B spins and an r^{-3} interaction law. Different interaction laws, and situations which involve some degree of correlation in the selection of B -spin sites lead to different forms for the function $E(2\tau)$ (see Appendix C).

a simple and manageable fashion. It may be rationalized by supposing that each relaxing B spin is in close contact with the lattice and is perturbed during one relaxation period by many small fluctuations occurring in the phonon spectrum. If these perturbations are all of comparable magnitude, then, according to the central limit theorem, one might expect their combined effect to give a random variable with a Gaussian distribution of values.¹³ This argument appears plausible enough where, as in the Raman process, the interaction involves a large number of lattice modes. However, it is not clear that it is appropriate in a case such as that of lattice relaxation by an Orbach process (which involves phonons with energy $\gg kT$).¹⁴ In order to bring out the importance of the assumption regarding the nature of the relaxation process we consider an alternative model for the time dependence of $\mu_j(t)$. Instead of assuming that $\mu_j(t)$ changes in many small steps we assume that it makes sudden jumps between the values $\pm \frac{1}{2}g_B\beta$. This manner of making the change represents an opposite extreme from the Gaussian behavior assumed earlier, and the predictions of this "sudden-jump" model can to some extent be looked upon as constituting a second limiting case. The Markoffian assumption, i.e., the assumption that the probability of a change in $\mu_j(t)$ is dependent only on the immediately preceding state, is retained, and leads to a time correlation for $\langle \mu_j(t')\mu_j(t'') \rangle$ as in Eq. (11).¹⁵

The distinction between Gaussian and sudden-jump models is unimportant in the case where $R\tau \gg 1$. Since each $\mu_j(t)$ switches a number of times between its two values, the integral $\xi_j(t)$ of Eq. (8a) consists of numerous accumulations of phase, all of them of comparable magnitude, and the central limit theorem can be used to justify the treatment of $\xi(t)$ as a Gaussian random variable. If however $R\tau \ll 1$, $\xi(t)$ will not approximate to a Gaussian random variable unless the local field variations are also Gaussian. This is clearly not the case for the field components due to individual B spins. Moreover, it is not even possible to argue that the resultant local field is a Gaussian variable. Since there is a wide disparity between the magnitudes of the local field components the central limit theorem is not applicable. Klauder and Anderson (Ref. 1) have adopted a different approach to the problem and have calculated the A -spin phase memory according to the sudden-jump model in the limit $R\tau \ll 1$, by considering B -spin

¹³ It is the accumulated phase in the integral $\xi(t)$ rather than the magnetic moment $\mu_j(t)$ which has to satisfy the conditions of the central limit theorem. $\mu_j(t)$ is itself clearly not a Gaussian variable for large t since its eventual distribution of values for large t is limited by the values $\pm \frac{1}{2}g_B\beta$.

¹⁴ In the Orbach process [R. Orbach, Proc. Roy. Soc. (London) **264**, 458 (1961)] relaxation is effected by making transitions to excited states which may be located many times kT above the ground state. The rate is then limited by the low density of energetic phonons in the lattice and the actual transition time is short compared with T_1 .

¹⁵ The time correlation function for the sudden-jump case is derived in C. P. Slichter, *Principles of Magnetic Resonance* (Harper and Row, New York, 1963), Appendix B.

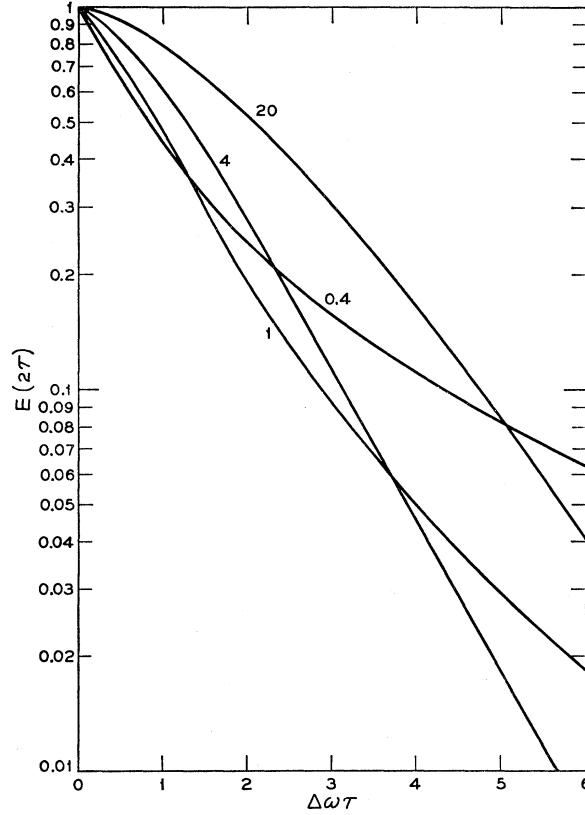


FIG. 1. Two-pulse echo decay functions $E(2\tau)$ calculated according to the Gauss-Markoff model [Eqs. (21) and (13)]. The numbers above the curves denote the ratio $\Delta\omega_{1/2}/R$ between the local field parameter and the B -spin relaxation rate. The curves are plotted in dimensionless form by taking $\Delta\omega_{1/2}\tau$ as the abscissa. Approximations which are valid in the limits $R\tau \ll 1$ or $R\tau \gg 1$ are given in Eqs. (25) and (26).

flips to cause a "diffusion" of the local field values. The argument is briefly as follows. Suppose that a small number of randomly selected B spins reverse their orientations in a time $\Delta t \ll 1/R$. This is equivalent to the insertion of $n_B R \Delta t$ moments each with $\mu_z = g_B\beta$ at random sites in the lattice. Using the statistical argument of Appendix A it can be seen that this causes a spin packet with initial frequency ω_0 to broaden out into a distribution¹⁶

$$K(\omega - \omega_0, \Delta t) = \frac{(2R\Delta\omega_{1/2}\Delta t)/\pi}{(\omega - \omega_0)^2 + (2R\Delta\omega_{1/2}\Delta t)^2}. \quad (28)$$

In the next time interval Δt there are $n_B R \Delta t$ additional spin flips at *unrelated sites*, and each frequency component in (28) gives rise to a new Lorentzian distribution. The change in local fields seen by the full ensemble of A spins can thus be represented as a diffusion process characterized by a Lorentz kernel and having a width

¹⁶ The factor 2 occurs here because each spin flip corresponds to the introduction of a new moment $\pm g_B\beta$, whereas in Appendix A the line broadening is calculated by assuming a random distribution of moments $\pm \frac{1}{2}g_B\beta$.

which increases linearly with time. Klauder and Anderson then show that the phase-memory function is proportional to $\exp(-m\tau^2)$ or, in our notation, $E(2\tau) = \exp\{-(2R\Delta\omega_{1/2}\tau^2)\}$. This can be written in the form

$$E(2\tau) = \exp\{-(2\tau/T_M)^2\}, \quad (29a)$$

where

$$T_M = 1.41(R\Delta\omega_{1/2})^{-1/2}, \quad R\tau \ll 1. \quad (29b)$$

The diffusion kernel (28) can be modified so that for long times it leads to a stationary distribution with width $\Delta\omega_{1/2}$ by writing

$$K(\omega - \omega_0, T) = \frac{\Delta\omega_{1/2}(1 - e^{-2RT})/\pi}{(\omega - \omega_0)^2 + \{\Delta\omega_{1/2}(1 - e^{-2RT})\}^2}. \quad (30)$$

It is doubtful, however, whether the resulting diffusion kernel can be used in conjunction with the Klauder and Anderson treatment. In making the repeated convolutions which are required in order to derive the two-pulse decay function $E(2\tau)$, it is implicitly assumed that individual A spins which have made larger-than-average frequency excursions in the past remain typical of the A -spin ensemble and will not have any specific tendency to make large excursions in the future. This assumption can be justified as long as $R\tau \ll 1$ since there is then only a small probability that a particular B -spin neighbor will make more than one flip. If an A spin sees an exceptionally large local field excursion during time $t \ll 1/R$, this may show that one or more of the nearer B spins have reversed their polarity during this time, but it does not indicate that the neighborhood contains more than a statistical number of B spins. There is therefore no special likelihood that the same A spin will undergo a large local field excursion during the next time interval Δt . The situation is quite different when $R\tau \gtrsim 1$. Spectral diffusion during τ may then involve multiple flips of the same B spins. A neighborhood which has shown large local field changes in a time $\sim 1/R$ is likely to contain more than the average number of B -spin neighbors and will therefore be characterized by larger local field changes throughout its future.¹⁷

Although neither the Gauss-Markoff nor the diffusion formulas for $E(\tau)$ are applicable if the B spins relax by sudden jumps and if $R\tau \sim 1$, it is still possible to set a lower limit on the phase-memory time for this case. The limit will represent a shortest possible value for the A -spin phase memory when it is controlled by B -spin relaxation. Let us suppose that all the B -spins flip simultaneously at the time $t = \tau$ when pulse II is applied. Since the echo signal amplitude depends on the difference between the A -spin phases accumulated in the two halves of the echo cycle (pulse I to pulse II,

and pulse II to the echo) this is the most extreme assumption we can make. The frequency deviation $\omega - \omega_0$ of A spin in the Lorentzian distribution $g_L(\omega) = (\Delta\omega_{1/2}/\pi) / \{(\omega - \omega_0)^2 + (\Delta_{1/2})^2\}$, which denotes the line broadening by B spins is then switched to $-(\omega - \omega_0)$, and the distribution of frequency changes $\Delta\omega$ is given by

$$g_L'(\Delta\omega) = (2\Delta\omega_{1/2}/\pi) / \{(\Delta\omega)^2 + (2\Delta\omega_{1/2})^2\}.$$

In the time τ following pulse II the precessing magnetization will decay according to the Fourier transform of $g_L'(\Delta\omega)$. Thus

$$E(2\tau)_{\min} = \exp\{-(2\Delta\omega_{1/2}\tau)\}, \quad (31a)$$

and

$$T_M(\min) = 1/\Delta\omega_{1/2}. \quad (31b)$$

It may be noted that this is approximately half the phase-memory time calculated on the Gauss-Markoff model [Eq. (27)].

The conclusions of this section may be summarized as follows. In the limit of $R\tau \gg 1$ (or $R \gg \Delta\omega_{1/2}$), $E(2\tau)$ is given by Eq. (24) and it does not matter which model is adopted for the B -spin relaxation process. If, on the other hand $R\tau \ll 1$ (or $R \ll \Delta\omega_{1/2}$), the time dependence assumed for $\mu(t)$ enters into the result. Assuming that $\mu(t)$ describes a random walk of many small steps we obtain Eq. (23); assuming $\mu(t)$ executes sudden jumps between $\pm \frac{1}{2}g_B\beta$ we obtain Eq. (29). The range $R\tau \sim 1$ is more difficult to treat than either of the limits above, but it is important, because it is here that the A -spin phase memory passes through its minimum. A very crude model gives $E(2\tau)$ as in (31a), but the result is probably only useful as a bounding value.

III. THREE-PULSE ECHOES—THEORY

In the three-pulse echo sequence τ denotes the time between pulses I and II, and T the time between pulses II and III. We are primarily concerned here with the decay function $D_T(\tau, T)$ (see Appendix B), which describes the echo signal attenuation factor associated with the physical processes taking place during the time T . As in Sec. II we can approach the problem of describing the time variation of μ_j the z -axis component of each B -spin moment, by adopting one of two models: the Gauss-Markoff model in which $\mu_j(t)$ is a Gaussian variable, and the sudden-jump model in which $\mu_j(t)$ switches at random times between the two values $\pm \frac{1}{2}g_B\beta$. In the limit $R\tau \ll 1$, $D_T(\tau, T)$ depends on "diffusion" of the local fields, and is given by the Fourier transform of the diffusion kernel (Appendix B). To find $D_T(\tau, T)$ according to the Gauss-Markoff model we have therefore to derive a diffusion kernel $K(\omega - \omega_0, T)$ by finding the statistical average of the resultant local fields when $\mu_j(t)$ is a Gaussian variable. The argument is a simple extension of that used in Appendix A to derive the linewidth due to static B -spin broadening.

¹⁷ On the Gaussian model an A spin in a dense B -spin neighborhood identifies itself much earlier. Many small steps will have been taken by each of the $\mu_j(t)$ even when $t \ll T_1$.

Instead of Eq. (A3) we have

$$K(\omega - \omega_0, T) = (2\pi)^{-1} \int_{-\infty}^{+\infty} d\rho \exp[-i\rho(\omega - \omega_0)] \\ \times \prod_{j=1}^N \left\{ (V^{-1}) \int dV_j \int d\mu_j \right. \\ \left. \times \exp[i\rho\gamma_A(1 - 3 \cos^2\theta_j)r_j^{-3}\mu_j(T)] f(\mu_j, T; \mu_{j0}) \right\}. \quad (32)$$

The variable ρ belongs to the integral form of δ function which is used here to apply the constraint $\sum \gamma_A(1 - 3 \cos^2\theta_j)r_j^{-3}\mu_j(T) = \omega - \omega_0$, and thus to extract from the sum the probability of finding a frequency shift $\omega - \omega_0$. The function $f(\mu_j, T; \mu_{j0})$ defines the distribution at time T of moments μ_j which at $T=0$ had the values μ_{j0} . It is shown elsewhere¹⁸ that

$$f(\mu_j, T; \mu_{j0}) = \frac{1}{\sigma[2\pi(1 - e^{-2R_jT})]^{1/2}} \\ \times \exp \left\{ -\frac{(\mu_j - \mu_{j0}e^{-R_jT})^2}{2\sigma^2(1 - e^{-2R_jT})} \right\}, \quad (33)$$

where R_j is a rate constant with the same meaning as in Eq. (11), and $\sigma^2 = \langle (\mu_j(0))^2 \rangle = \frac{1}{4}g_B^2\beta^2$. For our purpose we can drop the suffix on R and also use a somewhat simplified distribution,

$$f'(\mu_j', T) = \frac{1}{\sigma'[2\pi(1 - e^{-2RT})]^{1/2}} \exp \left\{ -\frac{\mu_j'^2}{2\sigma'^2(1 - e^{-2RT})} \right\}, \quad (34)$$

obtained by deleting the μ_{j0} term in (33). μ_j' in (34) stands for the change in μ_j from its initial value at $T=0$. This simplification is valid if, as we have assumed elsewhere, the shifts of the A -spin frequencies due to B -spin local fields are small compared with the static broadening (e.g., strain broadening) of the A -spin resonance line. At any point in the line where observations are made, the number of A spins with a B -spin neighbor whose moment μ_j is changing in one direction is then balanced by an equal number of A spins having a similar B -spin neighbor whose moment changing in the opposite direction. μ_j' is thus equally likely to have either sign and we can dispense with the asymmetric diffusion term $\mu_{j0}e^{-RT}$. [When $f(\mu_j, T; \mu_{j0})$ is replaced by the effective distribution $f'(\mu_j', T)$ the asymptotic width σ must also be modified to σ' but, since this parameter will be adjusted later to give agreement with the linewidth formula derived in Appendix A, the relation between σ and σ' need not be considered here.] By following the same steps as in Appendix A it can

be shown that Eq. (32) leads to a result

$$K(\omega - \omega_0, T) = (2\pi)^{-1} \int_{-\infty}^{+\infty} e^{-n_B V'} e^{-i\rho(\omega - \omega_0)} d\rho, \quad (34a)$$

where

$$V' = 2\pi \int_0^\infty r^2 dr \int_{-1}^{+1} d(\cos\theta) \\ \times \int d\mu' \{ 1 - \exp[i\rho\gamma_A \mu'(1 - 3 \cos^2\theta)/r^3] \} f'(\mu', T). \quad (34b)$$

Integrating first with respect to r, θ , and then with respect to μ' we find that

$$V' = (8/9)(2\pi^3/3)^{1/2} \gamma_A \sigma' (1 - e^{-2RT})^{1/2}. \quad (35)$$

At this point it is convenient to set $\sigma' = \frac{1}{2}(\pi/2)^{1/2} g_B \beta$ so that (34a) and (35) give the results (A6) and (A7) when $T \rightarrow \infty$, i.e., so that each spin packet eventually diffuses to give the linewidth function derived in Appendix A. Then $n_B V' = |\rho| \Delta\omega_{1/2} (1 - e^{-2RT})^{1/2}$ and

$$K(\omega - \omega_0, T) = \frac{\Delta\omega_{1/2} (1 - e^{-2RT})^{1/2} / \pi}{(\omega - \omega_0)^2 + \Delta\omega_{1/2}^2 (1 - e^{-2RT})}, \quad (36)$$

where $\Delta\omega_{1/2}$ is the half-width given in Eq. (A9). The decay factor is given by the Fourier transform

$$D_T(\tau, T) = \exp[-\Delta\omega_{1/2}\tau(1 - e^{-2RT})^{1/2}] \quad (37)$$

and, in the limit $RT \ll 1$ (given the previous condition $R\tau \ll 1$) we have

$$D_T(\tau, T) = \exp[-(2R)^{1/2} \Delta\omega_{1/2} \tau T^{1/2}]. \quad (38)$$

The diffusion function $K(\omega - \omega_0, T)$ in Eq. (36) is Lorentzian and has the property of retaining its form under repeated convolution, but it does not belong to the "homogeneous Markoffian" class of functions discussed by Klauder and Anderson (Ref. 1). The function $f(\mu_j, T; \mu_{j0})$ does belong to this class, but the property disappears when an average is taken over the different B -spin environments. The physical reasons why a homogeneous Markoffian function is not appropriate here are similar to those suggested in Sec. II after Eq. (30) and in Footnote 17. If $\mu_j(t)$ describes a random walk of many small steps as in the Gauss-Markoff model then, even in the earliest stages of spectral diffusion, there will have been some separation of the A spins according to their B -spin environments. A spins whose frequency has shifted over a relatively large interval in a time Δt will generally be those with more B spins in the immediate vicinity, and they will therefore have a tendency to undergo larger frequency shifts in subsequent time intervals.

Considerations of this kind lead one to question the validity of the initial assumption that the over-all

¹⁸ See Ref. 3, p. 152 for references and discussion.

three-pulse decay function can be written in the form of a product $D_r(\tau)D_T(\tau, T)$, and that the two factors can be calculated separately by considering the whole A -spin ensemble in each case. Although this factoring can be justified for the sudden-jump model in the limit of $R\tau \ll 1$ and $RT \ll 1$, it is not strictly applicable for any range of $R\tau$ or RT in the Gauss-Markoff case, since the decay $D_r(\tau)$ which occurs in the interval between pulses I and II will amount to the preferential elimination of those A spins which have most nearby B -spin neighbors. The magnetization pattern $M_x \sim \cos \omega_d \tau$ at the beginning of the time interval T will therefore characterize A spins which have less than the statistical number of B -spin neighbors, and it is for this group of A spins rather than for the complete ensemble that the factor $D_T(\tau, T)$ should be calculated. We shall not attempt to do this here, but merely note that three-pulse echo experiments may be less reliable than two-pulse experiments as a means of measuring local field changes. The effect of such a separation of A -spin environments would presumably be to reduce the decay rate during the time T , and to modify the Lorentzian kernel (36) in such a way as to cause it to resemble the more familiar Gaussian diffusion kernel.¹⁹

The diffusion kernel deduced from the sudden-jump model for the relaxation of B spins has been derived by Klauder and Anderson and is given in Sec. II, Eqs. (28) and (30). From the latter we derive the decay factor

$$D_T(\tau, T) = \exp[-\Delta\omega_{1/2}\tau(1 - e^{-2RT})], \quad (39)$$

which in the limit of $RT \ll 1$ becomes

$$D_T(\tau, T) = \exp[-2R\Delta\omega_{1/2}\tau T]. \quad (40)$$

The reasoning used in the derivation of the diffusion kernel (30) (and hence of the results above) again requires that the experimental linewidth should be several times larger than the linewidth $2\Delta\omega_{1/2}$ due to local fields. This must be so in order to ensure that each spin packet in the resonance line consists of A spins with a typical distribution of B -spin configurations in their neighborhood. The same condition is required for the derivation of the diffusion kernel according to the Gauss-Markoff model.

In the opposite limit of $R\tau \gg 1$ no spectral diffusion can be brought about by changes in the local fields due to the B spins since the full range of values of these fields has already been seen by the A spins before pulse II. $D_T(\tau, T)$ will therefore be independent of T except insofar as other processes, such as lattice relaxation of the A spins themselves, play a significant role. Under these circumstances it is not appropriate to

¹⁹ With the elimination of A spins having nearby B spins the local fields tend to be dominated by the relatively large number of B spins at intermediate distances which give local field interactions of comparable size. Changes in the local field may then be expected to approximate more closely to the pattern of a Gaussian random walk.

picture the A -spin resonance line as consisting of a number of slowly diffusing spin packets. It is more realistic to regard it as an assembly of nondiffusing spin packets, each homogeneously broadened and each having the line shape which is approximately given by the Fourier transform of $E(t)$,²⁰ where $E(t)$ is obtained by setting $2\tau = t$ in Eq. (26). A numerical computation of the cosine transform

$$\int_{-\infty}^{+\infty} \exp[-|(t/T_M)^{1/2}|] e^{i\omega t} dt$$

is shown in Fig. 2. The width parameter $\omega_N = 1/T_M = 1.8\Delta\omega_{1/2}^2 R^{-1}$. As $R\tau$ becomes smaller the spin packets will widen until at $R\tau \sim 1$ they have a homogeneous width $\sim \Delta\omega_{1/2}$.

IV. EXPERIMENTAL

The data was obtained with an electron-spin-echo spectrometer operating at 9.4 Gc/sec. Details of the apparatus have been reported elsewhere.²⁰ Measurements were made in the temperature range from 1.6 to 20°K, the portion of the range above 4.2°K being reached by transferring cold helium gas.²¹ Temperatures above 4.2°K were measured with a calibrated resistance thermometer. Two samples were studied in detail. Both were CaWO_4 crystals, one doped with Ce and Er, the other doped with Mn and Er. The concentrations were $[\text{Ce}] = 2 \times 10^{18}$ spins/cc, $[\text{Er}] = 2.5 \times 10^{18}$ spins/cc in one sample, and $[\text{Mn}] \approx 3.0 \times 10^{16}$ spins/cc, $[\text{Er}] = 1.1 \times 10^{18}$ spins/cc in the other.²² The

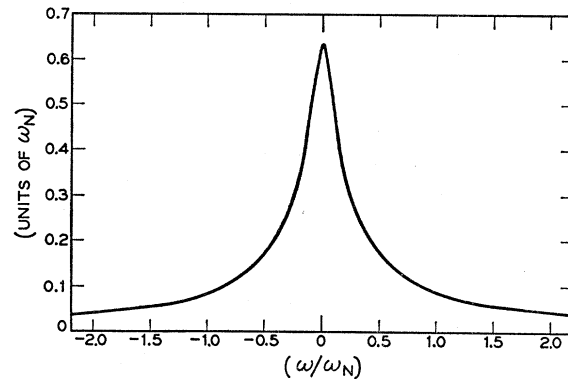


FIG. 2. Fourier transform of the two-pulse echo decay function $E(2\tau)$ calculated for the limiting case of $R\tau \gg 1$ [Eq. (26)]. The normalizing width is $\omega_N = 1/T_M$, where $T_M = 0.56R/(\Delta\omega_{1/2})^2$. R is the B -spin relaxation rate and $\Delta\omega_{1/2}$ the local field parameter. If $R/\Delta\omega_{1/2} \gg 1$ the "narrowing" conditions hold, Eq. (26) is a good approximation for $E(2\tau)$, and the above curve gives the spectrum of a spin packet in the resonance line.

²⁰ W. B. Mims, Rev. Sci. Instr. **36**, 1472 (1965).

²¹ The apparatus used for this is described by A. Kiel and W. B. Mims, Phys. Rev. **161**, 386 (1967).

²² In pure CaWO_4 there are 1.26×10^{22} Ca^{2+} ions/cc. The Mn concentration in the (Ca, Mn, Er) WO_4 sample was found by comparing signal strengths of Mn^{2+} and Er^{3+} . Er concentrations were obtained by optical-emission spectroscopic analysis. The Ce concentration in (Ca, Ce, Er) WO_4 was deduced by K. Nassau from a consideration of the crystal-growing conditions.

paramagnetic ions Ce^{3+} , Er^{3+} , and Mn^{2+} substitute at the Ca^{2+} site where the point symmetry in the host material is S_4 . All of the more intense lines belonged to axial sites. Nonaxial spectra (due to charge compensation of the trivalent ions at nearby lattice sites) were relatively weak. These doubly doped samples were chosen so that an A -spin group consisting of Ce^{3+} or Mn^{2+} ions could be studied while the Er^{3+} ions, constituting the B -spin environment, relaxed to the lattice. In addition to this, however, some measurements were made under experimental conditions such that Ce, Mn, or Er each played A - and B -spin roles simultaneously.

The ground states of Er^{3+} in CaWO_4 is a Kramers doublet with $g_{\parallel}=1.2$ and $g_{\perp}=8.3$. The relaxation times for Er as a function of lattice temperature T_L are shown in Fig. 3. At the upper end of the temperature range they were deduced from lifetime broadening of the resonance line, at the lower end they were measured by pulse recovery methods. $(\text{Ca}, \text{Er})\text{WO}_4$ is, unfortunately, a difficult system to study by any of the methods usually employed to measure lattice relaxation. It was chosen here only because of its very rapid variation of relaxation rate in the low-temperature range, which makes it a useful B -spin system for investigating the

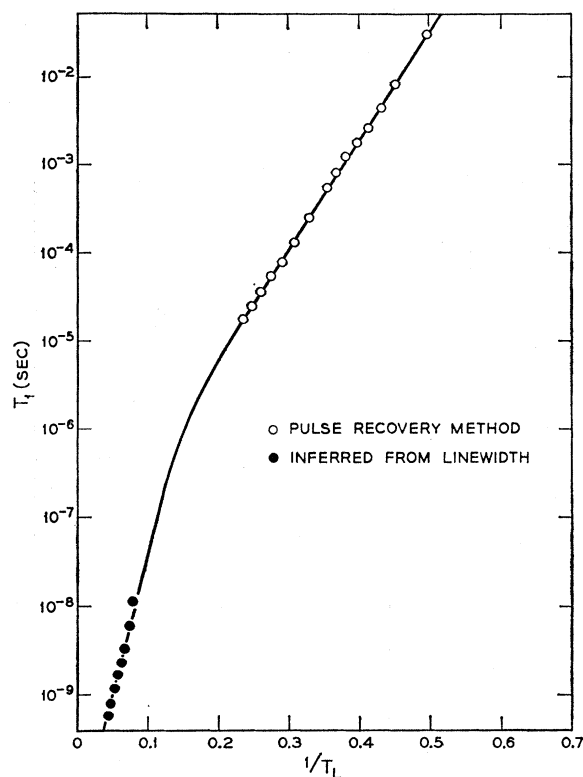


FIG. 3. Lattice relaxation times T_1 for Er^{3+} with H_0 along the c axis. For lattice temperature $T_L \leq 4.2^\circ\text{K}$ measurements were made by a pulse recovery method. In the upper part of the temperature range the times were inferred from the broadening of the resonance line (see text). The results can be fitted by two Orbach processes with characteristic temperatures $\Theta=30$ and 70°K .

two conditions $T\tau \ll 1$ and $R\tau \gg 1$ discussed earlier. At the lower end of the range, serious cross-relaxation effects were encountered, the times in Fig. 3 representing the longest observed decay components.²³ Some degree of uncertainty also prevails in the upper part of the range. In the straightforward case of lifetime broadening due to direct process relaxation between two levels we should expect to find $T_1=1/2W$, where W is the transition probability (in the limit of $\hbar\omega \ll kT$) and $2W$ is the full width at half-height (in rad/sec) corresponding to the lifetime broadening. It seems likely, however, that Er^{3+} relaxation occurs by way of the Orbach process.¹⁴ Transitions from the ground doublet to the upper states followed by a return to the *same level of the ground doublet* will then contribute to W but not to T_1 . In order to derive T_1 from the linewidth we should need to know the branching ratio for the transitions involving the two doublets. In default of this information we have arbitrarily assumed that the transition matrix elements are equal and taken T_1 to be twice the reciprocal of the full width at half-height. The results in Fig. 3 do not therefore constitute a highly accurate measurement of the relaxation times of Er^{3+} , are probably good to within a factor of two and will serve for our present purpose. The curve in Fig. 3 has been drawn on the assumption that the relaxation rate is controlled by two Orbach processes with characteristic temperatures $\Theta_1 \approx 30^\circ\text{K}$ and $\Theta_2 \approx 70^\circ\text{K}$. It was not possible to fit the results with a Raman process T^n curve, and the Orbach process appears to be the most likely relaxation mechanism in this case.²⁴ However, in view of the limited number of data obtained, the line in Fig. 3 should be regarded here rather as a means of interpolating between the high-temperature and low-temperature measurements than as a theoretical fit explaining the results.

The ground state of Ce^{3+} is a Kramers doublet with $g_{\parallel}=2.92$ and $g_{\perp}=1.43$. Measurements of the relaxation rate are reported in Ref. 21. In the lower part of the temperature range, Ce relaxation is slow compared with Er relaxation and has no effect on Ce or Er phase memories in the mixed sample. The upper part of the temperature range, in which the Ce spins act as the controlling B -spin environment (or undergo lattice relaxation before being able to contribute to the echo), is the only range of interest here. Relaxation is by way of a Raman process and gives times $\sim 40 \mu\text{sec}$ at $\sim 9^\circ\text{K}$.

²³ Cross-relaxation difficulties remained even when the field-sweep method described in Ref. 21 was used, probably because the available field sweep (~ 50 G) was not adequate to cover the whole of the Er line (70 G full width at half-height). Cross relaxation from hyperfine lines in the Er spectrum was also observed. The reasons for this large degree of cross relaxation are not known. It is difficult to see how the energy transfers could span such large intervals in times ~ 1 msec and at concentrations $\sim 0.01\%$ if only the dipolar fields of Er spins ($\gtrsim 1$ G) were involved in the cross-relaxation mechanism.

²⁴ Some spectroscopic results obtained by D. L. Wood (unpublished) indicate that there may be levels corresponding to $\Theta=35^\circ\text{K}$ and $\Theta=90^\circ\text{K}$ in $(\text{Ca}, \text{Er})\text{WO}_4$.

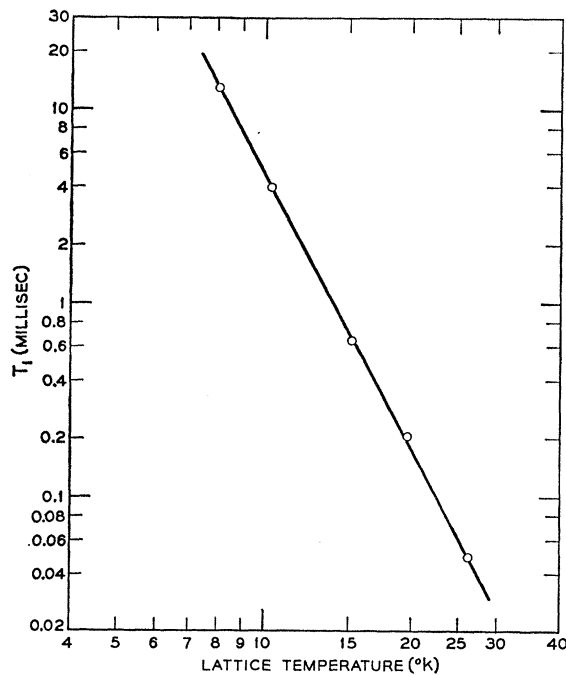


FIG. 4. Lattice relaxation times T_1 observed for one of the $M_s = +\frac{1}{2} \rightarrow -\frac{1}{2}$ transitions of Mn^{2+} in $CaWO_4$ with H_0 along the c axis. In the range shown $T_1 \propto T_L^{-\alpha}$, where T_L is the lattice temperature and $\alpha \approx 4.8$.

The paramagnetic resonance of Mn^{2+} in $CaWO_4$ is described by Hempstead and Bowers.²⁵ There are thirty allowed ESR transitions, and a formulation in terms of more than one relaxation time would be needed to describe the relaxation process fully. This would, of course, complicate the problem of calculating phase memories. We have not, however, attempted to investigate this situation in detail here, and the lattice relaxation measurements on Mn have been made merely in order to have an approximate check on the phase-memory observations for $(Ca, Mn, Er)WO_4$ in the upper part of the temperature range. The recovery times from spin inversion for one of the $M_s = \frac{1}{2} \rightarrow -\frac{1}{2}$ transitions have been measured and are shown in Fig. 4.²⁶ Over this temperature range, the results could be approximated by a T^5 law.

Figure 5 shows the phase-memory time for Ce in the $(Ca, Ce, Er)WO_4$ sample as a function of temperature. The g_{\perp} position was chosen since in the g_{\parallel} position and at our experimental frequency, the "nuclear modulation effect"²⁷ makes it difficult to determine the Ce phase memory. Figure 5 can be used to illustrate the various processes which predominate in the different temperature ranges. Somewhere below point P the spin-

²⁵ C. F. Hempstead and K. D. Bowers, Phys. Rev. **118**, 131 (1960).

²⁶ There were no problems due to spectral diffusion within the measured line. It was possible to invert the line under approximate 180° pulse conditions, and without a field sweep.

²⁷ L. G. Rowan, E. L. Hahn, and W. B. Mims, Phys. Rev. **137**, A61 (1965).

flip rate of Ce spins with resonant Ce spins and Er spins with resonant Er spins accounts for a major portion of the local field fluctuations and limits phase memory.²⁸ This could be called the " T_2 -limited" region.²⁹ From P to Q, $T_1(Er)$ controls $T_M(Ce)$. Since $R\tau < 1$ here, the phase memory becomes shorter as the Er relaxation rate increases. At Q, $T_1 \sim \tau \sim 1/\Delta\omega_{1/2}$. From Q to R, $T_1(Er)$ still controls $T_M(Ce)$, but $R\tau > 1$, and $T_M(Ce)$ lengthens as $T_1(Er)$ shortens. From R to S, $T_1(Ce)$ is the limiting factor. At the beginning of the range RS, $T_1(Ce)$ acts mainly via the local fields, i.e., some Ce spins act as B spins in relation to others. At the end, $T_M(Ce)$ is limited by the lattice relaxation of those cerium spins which would otherwise contribute to the echo. Since the Ce relaxation takes place between the two levels of the ground doublet and does not involve real transitions to other levels we should expect that $T_1(Ce) \rightarrow T_M(Ce)$ in this limit, T_M being a true transverse relaxation time T_2 in the sense of the Bloch equations. The phase memory of the Er component in the sample follows a similar curve as far as S but does not, of course, lengthen again after this point is reached. Beyond S, $T_M(Er) \sim T_1(Er)$. (If a third paramagnetic species with longer relaxation times and less strongly temperature-dependent relaxation behavior were doped into the sample we might expect to find two minima in its phase-memory curve at points where Er and Ce fulfilled the condition $T_1 \sim 1/\Delta\omega_{1/2}$.)

Experimental values for $T_M(Ce)$ at temperatures in the middle of the regions PQ, QR, RS, and at the

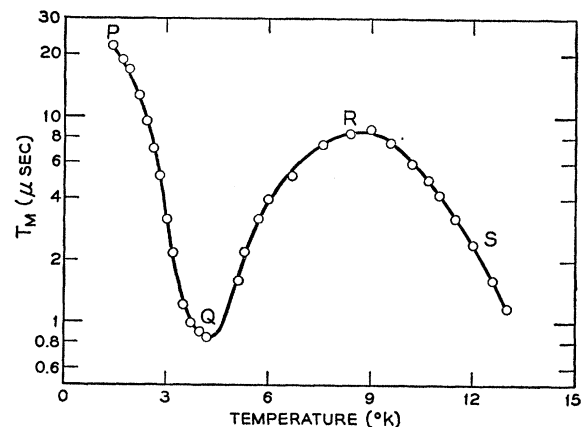


FIG. 5. Phase-memory time T_M as a function of temperature for Ce in a double-doped $(Ca, Ce, Er)WO_4$ sample with H_0 in the ab plane. T_M is defined as the time between pulse I and the echo required to produce an e^{-1} reduction in the echo amplitude. The letters PQRS indicate temperatures at which changes occur in the manner in which T_M is controlled.

²⁸ The phase memory was still lengthening slightly between 1.8 and 1.6°K and it is not certain that the T_2 -limited region was reached at point P. Some temperature dependence may of course be found even in the T_2 -limited region if $\hbar\omega \sim kT$.

²⁹ In this context T_2 would mean the time for a spin flip to occur and not the phase-memory time. T_M would be limited by local field noise and would not be a measure of the rate of flip-flop processes.

TABLE I. Comparisons between experimental and calculated phase-memory times T_M for the Ce spin system in the (Ca, Ce, Er)WO₄ sample with H_0 in the ab plane. T_M is controlled by local field fluctuations in the sample. For the first four results the principal source of these fluctuations is lattice relaxation of the Er spin system. At 10°K local field averaging has reduced the effects of Er relaxation, and the dominant fluctuations are due to relaxation of the Ce spin system. $\Delta\omega_{1/2}$ is a measure of the local fields involved. Calculations are made according to two models as described in the text. The calculations depend on the order of magnitude of $R\tau$ where R is the relevant lattice relaxation rate and 2τ is the duration of the spin-echo cycle of events. R values for Er are taken from Fig. 3. The R value for Ce is extrapolated from a curve given in Ref. 21. A curve showing T_M as a function of the lattice temperature is given in Fig. 5. Decay curves for two- and three-pulse echoes at the 2.2°K point are shown in Figs. 6 and 7.

B-spin system	Lattice Temp (°K)	1/R (μsec)	$\Delta\omega_{1/2}$ (mrad/sec)	T_M (expt.) (μsec)	T_M (calc) (μsec)	Method of calculation	$R\tau$	Equation
Er	2.2	8×10^8	6.1	13.0	11.4	Gauss-Markoff	$\ll 1$	(25b)
					51.0	sudden jump	$\ll 1$	(29b)
Er	2.4	2.5×10^8	6.1	10.4	7.7	Gauss-Markoff	$\ll 1$	(25b)
					28.5	sudden jump	$\ll 1$	(29b)
Er	4.2	18	6.1	0.86	0.3	$1.8/\Delta\omega_{1/2}$	~ 1	(27a)
					68.0	$3.8/R$	~ 1	(27b)
Er	6.0	1.8	6.1	4.0	0.0084	Gauss-Markoff	$\gg 1$	(26b)
Ce	10.0	15	0.84	6.7	5.8	Gauss-Markoff	$\ll 1$	(25b)
					6.0	sudden jump	$\ll 1$	(29b)

minimum Q are given in Table I. Values calculated on the Gauss-Markoff and sudden-jump models are shown for comparison, the relevant formulas being indicated in the last column. The orientation is with $H_0 \perp$ the c axis. A value $T_1(\text{Ce}) = 15 \mu\text{sec}$ at 10°K, required in order to calculate $T_M(\text{Ce})$ at the point chosen in the RS range, was obtained by extrapolating from the curve in Ref. 21, Fig. 6. Values of $T_1(\text{Er})$ for H_0 in the ab plane have been taken from Fig. 3, where the values for $H_0 \parallel$ to the c axis are given. One cannot be

entirely certain that parallel and perpendicular relaxation times are the same, although one would expect the relaxation rate to be very nearly isotropic if governed by the Orbach process. The assumption does not, in any case, appear to lead to large errors at the lower temperatures (although here anisotropy of T_1 would be more likely to occur because of a possible admixture of direct process relaxation). At 6°K, on the other hand, the result strongly suggests that a smaller value of T_1 should be used. It may also be noted that the expression $1.8/\Delta\omega_{1/2}$ leads to the correct

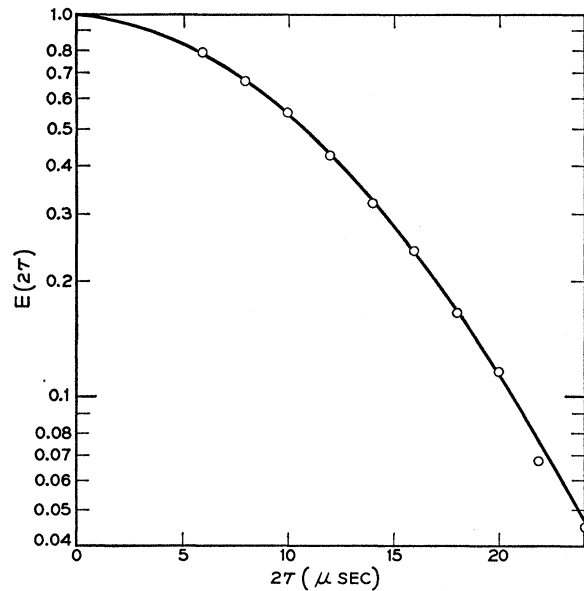


FIG. 6. Two-pulse decay envelope $E(2\tau)$ for Ce in the (Ca, Ce, Er)WO₄ sample with H_0 in the ab plane. The lattice temperature is 2.2°K. The experimental decay curve can be approximately represented by the function $E(2\tau) = \exp\{-(2\tau/T_M)^x\}$, where $x=1.9$ and $T_M=13 \mu\text{sec}$.

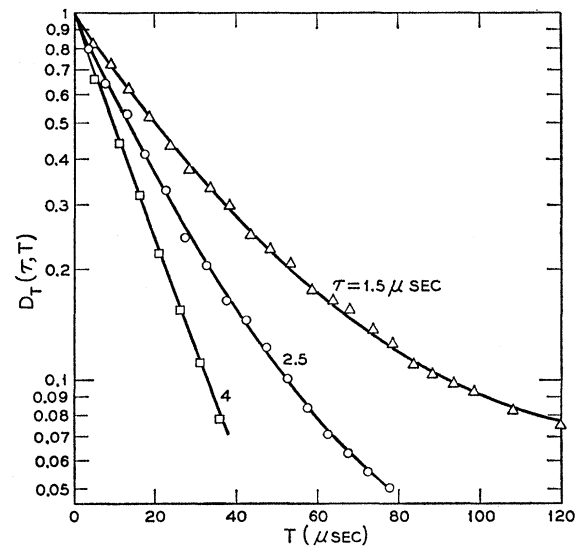


FIG. 7. Experimental plots of the three-pulse decay function $D_T(\tau, T)$ for Ce in the (Ca, Ce, Er)WO₄ sample, with H_0 in the ab plane. The lattice temperature is 2.2°K. The experimental curves can be approximately represented by a decay function $D_T(\tau, T) = \exp(-c\tau^u T^v)$, where $u=0.87$, $v=0.91$, and $c=0.029$, τ and T both being expressed in μsec .

TABLE II. Comparisons between experimental and calculated phase-memory times T_M for the Mn spin system in the (Ca, Mn, Er)WO₄ sample with $H_0 \parallel$ to the c axis. The situation is analogous to that summarized in Table I and the variation of T_M with temperature similar to that shown in Fig. 5. The R values for Er are taken from Fig. 3, and the R value for Mn from Fig. 4. The two-pulse echo decay curve at the 7.65°K point is shown in Fig. 8. At 4.2°K the echo could not be detected. (It is difficult to see echo signals due to weak resonance lines with the apparatus used here when $T_M \leq 1$ μ sec.)

B -spin system	Lattice temp (°K)	$1/R(B)$ (μ sec)	$\Delta\omega_{1/2}$ (mrad/sec)	T_M (expt) (μ sec)	T_M (calc) (μ sec)	Method of calculation	$R\tau$	Equation
Er	2.08	15×10^3	0.55	46	70	Gauss-Markoff	$\ll 1$	(25b)
					234	sudden jump	$\ll 1$	(29b)
Er	2.5	1.7×10^3	0.55	23	34	Gauss-Markoff	$\ll 1$	(25b)
					79	sudden jump	$\ll 1$	(29b)
Er	~ 4.2	18	0.55	≤ 1	3.3	$1.8/\Delta\omega_{1/2}$	~ 1	(27a)
Er	6.6	0.9	0.55	9.5	2.1	Gauss-Markoff	$\gg 1$	(26b)
Er	7.65	0.2	0.55	42	9.4	Gauss-Markoff	$\gg 1$	(26b)
Mn	17.25	350	0.025	48	154	Gauss-Markoff	$\ll 1$	(25b)
					168	sudden jump	$\ll 1$	(29b)

order of magnitude for T_M at the minimum at 4.2°K, but that $3.8/R$ gives a value which differs from the experimental value here by a factor of 80. If we tentatively assume the validity of Eq. (27b) at 4.2°K and of Eq. (26b) at 6°K, and then use the experimental values of T_M to deduce $T_1(\text{Er})$, we obtain $T_1(\text{Er}) = 0.23$ μ sec at 4.2°K and $T_1(\text{Er}) = 0.0038$ μ sec at 6°K.³⁰ The form of the two- and three-pulse decay functions was investigated at 2.2°K (i.e., in the PQ region where $R\tau \ll 1$, and where calculations of T_M give the right order of magnitude). The two-pulse decay envelope at 2.2°K is shown in Fig. 6. It can be fitted by the function $E(2\tau) = \exp\{- (2\tau/T_M)^x\}$, where $x = 1.9$ and $T_M = 13$ μ sec.³¹ The three-pulse decay measurements are shown as a function of T for several values of τ in Fig. 7. They can be roughly fitted by $D_T(\tau, T) = \exp(-c\tau^u T^v)$, where $u = 0.87$, $v = 0.91$, and $c = 0.029$ (if τ, T are in μ sec). The form of the decay functions is in somewhat better agreement with the sudden jump model than with the Gauss-Markoff model as can be seen by comparing $E(2\tau)$ with Eqs. (25a) and (26a), and $D_T(\tau, T)$ with Eqs. (38) and (40). The actual magnitudes of T_M lie closer to the predictions of the Gauss-Markoff model however (see Table I). The calculated value of the constant c in $D_T(\tau, T)$ is 0.097 according to the Gauss-Markoff model and 0.0015 according to the sudden-jump model (τ, T being in μ sec in both cases.)

³⁰ Measurements of $T_1(\text{Er})$ in the g_{\perp} position at somewhat lower temperatures make it seem unlikely that $T_1(\text{Er})$ could be as short as 0.23 μ sec at 4.2°K. The relaxation measurements, made at X -band, may not, however, be relevant in the present circumstances. When the Ce line is adjusted to give resonance at 9.4 Gc/sec in the g_{\perp} position, the Er resonance interval is 54.5 Gc/sec.

³¹ Earlier experiments performed with a (Ca, Ce, Er)WO₄ sample gave a decay curve $E(2\tau)$ of approximately the same form [Ref. 2, Figs. 5(a) and 6(a)]. Ce and Er concentrations in the earlier sample were each approximately 2.5 times less than in the present sample. Temperature and the resonance frequency were also somewhat different.

The phase memory for Mn²⁺ in the (Ca, Mn, Er)WO₄ sample showed a sequence of changes similar to that observed for (Ca, Ce, Er)WO₄. Measurements were made on one of the $M_s = -\frac{1}{2} \leftrightarrow +\frac{1}{2}$ lines with $H_0 \parallel$ to the c axis. The phase-memory times are shown in Table II and compared with calculated values as in the case of the (Ca, Ce, Er)WO₄ sample. Allowing for the uncertainty in the concentration and in the measurement of $T_1(\text{Er})$, the results at 2.08 and 2.5°K appear to be reasonably close to the values predicted according to the Gauss-Markoff model. Agreement is less good at 4.2°K. The disappearance of the Mn echo signal shows that $T_M \leq 1$ μ sec at the minimum. According to Eq. (31b), T_M cannot be less than $1/\Delta\omega_{1/2}$, and hence we deduce that $\Delta\omega_{1/2} \geq 10^6$, or at least twice the value given in Table II. This is probably larger than the error to be expected from the analysis. If, however, we assume $\Delta\omega_{1/2} = 10^6$, then according to the Gauss-Markoff model we obtain the estimates $T_M = 44$ μ sec at 2.08°K and $T_M = 21$ μ sec at 2.5°K, which are in better agreement with the experimental results than the estimates given in Table I. The discrepancies at 6.6 and 7.65°K are already large in Table II and would be increased still further by setting $\Delta\omega_{1/2} = 10^6$. If $\Delta\omega_{1/2} = 10^6$ an eighteen-fold increase in R is required to bring the experimental results into agreement with the calculated phase memories. Although $T_1(\text{Er})$ was only derived by interpolation in this temperature range, it is difficult to see how such very large values of R could be consistent with the values measured at higher and at lower temperatures. A possible anisotropy or field dependence of $T_1(\text{Er})$ cannot be invoked here as it was in the discussion of the cerium results, given $T_1(\text{Er})$ and $T_M(\text{Mn})$ were both measured in the g_{\parallel} position and at fields differing by a factor of only 1.5:1. The last result in Table II, showing the limitation of $T_M(\text{Mn})$ by Mn lattice relaxation, is within a factor ~ 3 of the estimate. This error could arise

from the approximate nature of the $T_1(\text{Mn})$ measurements, or from errors in estimating the concentration of Mn. It may be noted that the concentration of Mn depends on that of Er since it was determined by comparing the two spectra in the sample. If the Er concentration is revised upwards by a factor of two in order to bring $\Delta\omega_{1/2}$ for the Mn-Er broadening up to 10^6 and to give agreement in the earlier part of the Table, then $\Delta\omega_{1/2}$ will become 0.05×10^6 for the Mn-Mn broadening leading to the calculated values $T_M = 97 \mu\text{sec}$ (Gauss-Markoff) and $T_M = 119 \mu\text{sec}$ (sudden jump) at 17.25°K .

The high Mn dilution and the consequent weakness of Mn-Mn local fields (in contrast with the Ce-Ce local fields in the previous sample) made it possible to undertake a more careful study of the form of $E(2\tau)$ in the range of very rapid Er relaxation. The two-pulse envelope for Mn^{2+} at 7.65°K is shown in Fig. 8.³² It can be fitted by $\exp\{-(2\tau/T_M)^x\}$, where $x=0.7$ and $T_M=42 \mu\text{sec}$. A similar result was obtained at 6.6°K . At 11.85°K , $T_M=80 \mu\text{sec}$ and the decay curve was approximately exponential. The change of shape here is probably due to the onset of Mn-Mn local-field effects since above this temperature T_M begins to shorten. At 17.25°K the decay curve also appeared to give an almost exponential fit (over the first decade of measurements) but a careful study of the form of $E(2\tau)$ could not be made on account of poor signal-to-noise. A set of three-pulse decay measurements were made at 8.2 and 6.8°K . The signal-to-noise ratio was not good enough to yield the form of $D_T(\tau, T)$ as a

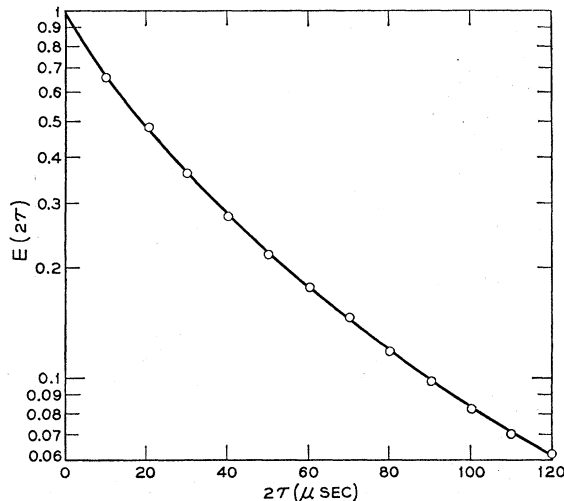


FIG. 8. Two-pulse decay envelope $E(2\tau)$ for one of the $M_s = +\frac{1}{2} \leftrightarrow -\frac{1}{2}$ lines of Mn^{2+} in the $(\text{Ca}, \text{Mn}, \text{Er})\text{WO}_4$ sample, with H_0 along the c axis. The lattice temperature was 7.65°K . The phase memory of Mn is controlled by lattice relaxation rate R of the Er^{3+} spins. $R\tau \gg 1$. Points can be fitted by $E(2\tau) = \exp\{-(2\tau/T_M)^x\}$, where $x=0.7$ and $T_M=42 \mu\text{sec}$.

³² Signal-to-noise for the Mn lines in the sample was poor and boxcar techniques were used to integrate the amplitudes of several hundred echo pulses.

TABLE III. Three-pulse echo decay for the $(\text{Ca}, \text{Mn}, \text{Er})\text{WO}_4$ sample in the range where $R\tau \gg 1$ [$R=1/T_1(\text{Er})$]. T_e is the time T for which $D_T(\tau, T) = e^{-1}$. The times show only a slight dependence on τ indicating that spectral diffusion has little if any effect on $D_T(\tau, t)$ when $R\tau \gg 1$.

Lattice temp. ($^\circ\text{K}$)	τ (μsec)	T_e (msec)
6.8	5	2.8
6.8	10	2.5
8.2	5	2.6
8.2	10	2.2
8.2	20	1.9

function of T but the times T_e giving an e^{-1} reduction in $D_T(\tau, T)$ and the corresponding values of τ are given in Table III. It can be seen that T_e is only weakly dependent on τ . Presumably the Er-Mn local field fluctuations have become too rapid to play any significant part in determining $D_T(\tau, T)$ as suggested at the end of Sec. III. The observed dependence on τ and T may be due to Mn-Mn interactions or to small residual changes in the mean local fields created by the Er spins.

No special effort was made to analyze the form of $E(2\tau)$ and $D_T(\tau, T)$ in the range $R\tau \ll 1$ for the Mn line in the $(\text{Ca}, \text{Mn}, \text{Er})\text{WO}_4$ sample, since a more satisfactory investigation of the behavior of the decay functions in this range could be made for the Er line (i.e., a line belonging to one of the more strongly doped species). The Er line in the $(\text{Ca}, \text{Ce}, \text{Er})\text{WO}_4$ sample in the g_{11} orientation formed a particularly convenient subject for this study. Signals were initially 30 to 40 dB above noise, the phase memories were relatively long, and the "nuclear modulation" effects negligible. Er spins acted as both A and B spins. The experimental conditions were such that the microwave pulses excited a spectrum of spin packets ~ 1.5 G wide, constituting $\sim 2\%$ of the total width of the line. 98% of the Er spins were thus foreign to the small group of A spins being observed, and stood in much the same relation to them as to the Ce or Mn spins in the previous experiments.³³ The Ce relaxation rate in the sample was approximately two orders of magnitude less than the relaxation rate of Er and had therefore no effect on the result. Spin-spin flips in the Ce system or in the Er system could also be ignored at the temperature where the studies were made, since T_M continued to lengthen as the temperature was reduced, indicating control of the phase memory by $T_1(\text{Er})$. The two-pulse decay function $E(2\tau)$ at 2.48°K is shown in Fig. 9. It can be fitted to $\exp\{-(2\tau/T_M)^x\}$ where $x=1.31$ and $T_M=11.9 \mu\text{sec}$. A similar curve was obtained at 2.85°K with $x=1.4$ and $T_M=8.4 \mu\text{sec}$. The

³³ This condition is not strictly necessary, since the same group of spins could play the roles of A and B spins.

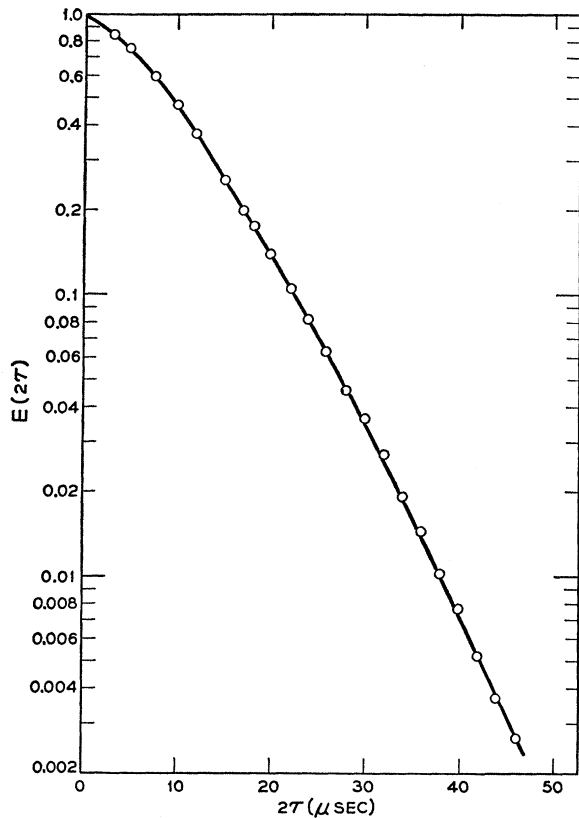


FIG. 9. Two-pulse decay envelope $E(2\tau)$ for Er^{3+} in the (Ca, Ce, Er) WO_4 sample with H_0 along the c axis. The lattice temperature is 2.48°K . Points can be fitted by $E(2\tau) = \exp\{- (2\tau/T_M)^x\}$, where $x=1.3$, and $T_M=11.9 \mu\text{sec}$.

calculated value of $\Delta\omega_{1/2}$ for Er-Er local fields in the sample in the g_{11} position is 7.4×10^5 rad/sec. The corresponding calculated values for T_M are 28.2 and 17.7 μsec according to the Gauss-Markoff model, and 69.3 and 34.5 μsec according to the sudden-jump model. The experimental results are thus smaller than those estimated according to either of the two models. This could possibly arise from an underestimate of the Er concentration, but there is little to suggest such a conclusion in the rest of the data obtained with this sample. [The experimental value of $T_M(\text{Ce})$ at the minimum (see Table I) is longer than the calculated value $1.8/\Delta\omega_{1/2}$ indicating that, if anything, the concentration may be lower than the estimated amount.] Experimental curves for $D_T(\tau, T)$ as a function of T at 2.48°K are shown in Fig. 10. $D_T(\tau, T)$ can be fitted by $\exp(-c\tau^u T^v)$, where $u=0.6$, $v=0.8$, and $c=0.039$ (if τ, T are expressed in μsec). The form of the decay functions $E(2\tau)$ and $D_T(\tau, T)$ does not approximate very closely to the prediction of either model, but the actual numerical magnitudes again give better agreement with the Gauss-Markoff model. The constant c in $D_T(\tau, T)$ is calculated to be 0.025 according to the Gauss-Markoff model and 0.00082 according to the sudden-jump model (τ, T being in μsec in both cases).

V. DISCUSSION

The general behavior of T_M as a function of temperature seems to be fairly easy to explain. Although only two instances of the spin-packet narrowing phenomenon, which causes T_M to lengthen as the temperature is raised, have been reported here, similar behavior has been observed in several different samples. Narrowing of this kind may be of some practical importance when either ENDOR, or measurements in which spin-echo techniques are applied, have to be performed with impure materials. The initial shortening of phase memory with rising temperature, as a resonant species begins to relax and to provide a fluctuating B -spin environment, is quite general and is the usual reason why electron-spin-echo experiments have to be performed at low temperatures. (T_M is often too short for echo experiments even when T_1 is still several μsec long.)

The actual decay times and the functional form of the echo envelope are harder to account for. By and large the Gauss-Markoff model for the time dependence of lattice relaxation appears to give better agreement than the sudden-jump model, but there are a number of major discrepancies between the experimental and calculated values of T_M which make it impossible to decide conclusively in favor of either model on the basis of the experimental evidence. The worst discrepancies seem to be associated with the values adopted for $T_1(\text{Er})$ in the range 4.2 – 12.5°K , suggesting that the interpolated values in Fig. 3 are at fault. Although it is hard to see how errors large enough to

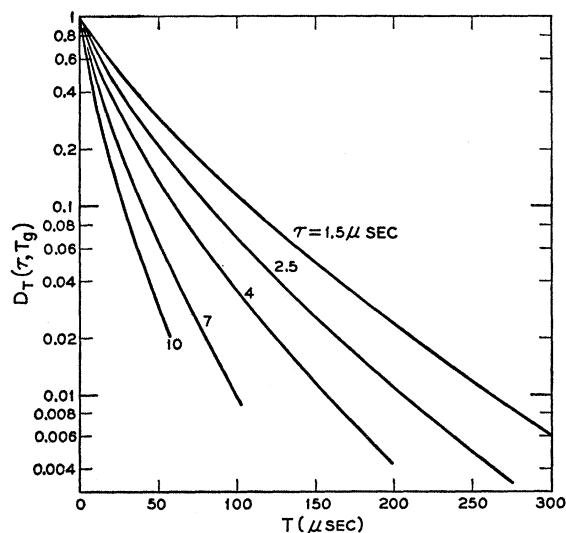


FIG. 10. Experimental plots of the three-pulse decay function $D_T(\tau, T)$ for Er in the (Ca, Ce, Er) WO_4 sample, with H_0 along the c axis. The lattice temperature is 2.48°K . The experimental curves can be approximately represented by a decay function $D_T(\tau, T) = \exp(-c\tau^u T^v)$ where $u=0.6$, $v=0.8$, and $c=0.039$, τ and T both being expressed in μsec . (Experimental points have been omitted in order to avoid clutter. Points fell on or close to the lines drawn, the accuracy being somewhat better than in the case of Fig. 7.)

account for the discrepancies could have arisen in either the measurements of T_1 , or in the interpolation, this at least provides a ready explanation for the T_M results. It should be pointed out, however, that this explanation is not the only possible one, and that the discrepancies may have a more interesting physical origin. The phase memory is regulated by the total rate at which transitions are occurring between the two levels of the Er ground doublet, whereas T_1 gives the net excess of transitions in one direction. The absolute transition rate and the net rate are normally related to one another in a simple manner, but this relation will break down if there is an energy-conserving transfer of excitation through the spin system. Such a transfer might for example occur if there were a "phonon bottleneck" in the relaxation process, many individual spins changing their orientation for each quantum of spin energy finally dissipated. In the present instance, a phonon bottleneck involving the Er ground doublet does not appear likely, but an alternative process involving the first excited state could lead to an equivalent result. Let us consider, for example, the following hypothetical sequence of events involving an energetic phonon and two nearby erbium ions Er(1) and Er(2). We denote the states belonging to the ground doublet as $|a(r)\rangle$, $|b(r)\rangle$ and one of the excited states as $|c(r)\rangle$. Let us begin with Er(1), Er(2) in states $|a(1)\rangle$, $|b(2)\rangle$. The energetic phonon first raises Er(1) to the state $|c(1)\rangle$, a flip-flop with Er(2) changes the states to $|b(1)\rangle$, $|c(2)\rangle$, and emission of a phonon by Er(2) leaves the system in states $|b(1)\rangle$, $|a(2)\rangle$. One phonon has caused two spins to change their states in the ground doublet. By generalizing from this sequence of events one can envisage a means by which a single energetic phonon might cause several Er ions to change their state in the ground doublet, the actual number depending on the probability for the $|a\rangle$ to $|c\rangle$, $|c\rangle$ to $|a\rangle$ (or $|b\rangle$ to $|c\rangle$, $|c\rangle$ to $|b\rangle$) flip-flop process as compared with the probability for emission and breakup of the phonon.³⁴ (This mechanism would be distinct from the usual flip-flop between spins of a ground doublet in that it would be strongly temperature-dependent, and would probably involve interactions other than the magnetic-dipole interaction such as, for example, the electrostatic quadrupole-quadrupole interaction.³⁵)

The results also show a somewhat unsatisfactory agreement with the predicted form of the decay functions, and indicate that there may be errors in the estimate of the local field parameters $\Delta\omega_{1/2}$. An error in $\Delta\omega_{1/2}$ could easily originate from an error in the

³⁴ We have no direct evidence for the existence of this process in (Ca, Er)WO₄, although it might, if present, help to account for the surprisingly high cross-relaxation rate mentioned in footnote 23. It would also contribute to the lifetime broadening of the microwave resonance line at higher temperatures, and might invalidate some of the deductions which were made in order to plot the $T_1(\text{Er})$ curve in Fig. 3.

³⁵ References are given in a paper by J. M. Baker and A. E. Mau, Can. J. Phys. 45, 403 (1966).

measurement of the B -spin concentration. This would, however, simply change the scale of the decay functions without altering their form. The form itself is sensitive to several other physical properties. One of them—the time evolution of the spin component $\mu_j(t)$ during lattice relaxation—has already been discussed in some detail. Two others must also be considered. There may be some degree of spin clustering in the sample, resulting from the thermodynamic conditions which obtained during the growth and annealing of the crystal,³⁶ and there may be a contribution to the spin-spin interaction (i.e., to the local field) arising from nonmagnetic-dipolar forces obeying a different radial law. These two causes would be hard to distinguish experimentally. Both would enter the statistical calculation in a similar way, so that a particular set of results might be interpreted either in terms of a modified law of interaction or in terms of a clustering density function $f(r)$ (see the end of Appendix A). The case of quadrupole-quadrupole interaction, which involves an r^{-5} interaction law, is outlined in Appendix C. The equivalent clustering function is $f(r) \propto r^{-6/5}$. For an r^{-5} law, the Gauss-Markoff model gives the results $E(2\tau) = \exp\{-(2\tau/T_M)^{9/10}\}$ when $R\tau \ll 1$, and $E(2\tau) = \exp\{-(2\tau/T_M)^{3/10}\}$ when $R\tau \gg 1$. The corresponding three-pulse result is $D_T(\tau, T) = \exp\{-c'\tau^{3/5}T^{3/10}\}$. These calculations serve to illustrate the sensitivity of decay functions to any deviation from ideal randomness in the substitution of ions or from the classical r^{-3} dipolar interaction law. Experiments on the Er line gave decay functions whose form agrees somewhat better with the predictions of the r^{-5} law than with the predictions of the r^{-3} law, suggesting that there is some slight admixture of nondipolar forces here (or alternatively, some tendency towards aggregation of the ions.) However, in view of the semiquantitative nature of the agreement obtained elsewhere in the experiments, it would be unwise to draw too definite a conclusion from this.

One may ask whether, eventually, the interpretation of phase-memory functions could not be made into a dependable method for extracting information regarding the properties of solids. Linewidth studies in NMR have proved to be useful in this way, and the echo technique, by eliminating the problems caused by the inhomogeneous broadening of ESR lines, should provide a method of at least as much versatility and power. Clearly, one requirement for an advance in this direction would be an improvement in the reliability of subsidiary measurements, as, for example, in the determination of concentrations and in the measurement of lattice relaxation times in the difficult range

³⁶ The samples were carefully annealed at temperatures just below the melting point, and there seems to be no good reason why the divalent Mn ions should not be substituted quite randomly in the lattice. One might, on the other hand, suspect clustering for Ce³⁺ or Er³⁺. Trivalent ions in CaWO₄ are normally compensated by a monovalent ion or by a Ca²⁺ vacancy. Some degree of association between the trivalent ions and the compensating centers is liable to result in an association between the trivalent ions themselves.

from 10^{-6} to 10^{-8} sec.³⁷ A more fundamental need, however, is for a rigorous treatment of the dynamics of a spin-phonon system. This, by either establishing the limits of validity for a Gauss-Markoff model or by suggesting a better alternative, could provide a reliable foundation for the statistical calculations which are involved in any analysis of the lattice relaxation effects.

ACKNOWLEDGMENTS

It is a pleasure to recognize here the contribution made by J. R. Klauder to this work, both by outlining the solution of the two-pulse problem according to the Gauss-Markoff model, and by helping to clarify various points in discussion. The author would also like to thank R. Gillen for performing some of the experimental measurements, and K. Nassau for growing the samples.

APPENDIX A. DIPOLAR BROADENING DUE TO RANDOMLY DISTRIBUTED PARAMAGNETIC CENTERS

At high magnetic dilutions one can ignore the crystal lattice and regard the paramagnetic ions as being randomly distributed throughout a volume V . Dipolar broadening can then be treated according to the statistical theory, developed by Margenau³⁸ and others for the purpose of explaining the broadening of spectral lines in gases. The argument reproduced below is essentially the same as that given by Anderson.³⁹ It is included here for convenience of reference, and in order to make it possible to abbreviate the derivations given elsewhere in the paper.

Let us suppose that the lattice contains unlike spin groups A and B , and that we have to find the broadening of the A resonance line due to the presence of the B spins. The only significant terms in the dipolar Hamiltonian are then the $S_{zi}(A)S_{zj}(B)$ terms and we can describe the interaction for a particular A spin in terms of the shift $\Delta\omega$ in its Larmor frequency where

$$\Delta\omega = \gamma_A \sum_j \mu_{Bj} (1 - 3 \cos^2\theta_j) / r_j^3, \quad (\text{A1})$$

r_j is the distance between the A spin and the j th B spin, and θ_j is the angle between the direction of the

Zeeman field H_0 and the line joining the two spins. γ_A is the gyromagnetic ratio $g_A\beta/\hbar$ for the A spins, and μ_{Bj} is the matrix element of $g_B\beta S_z^j$. The sum in (A1) can be interpreted as the local field at an A spin due to a particular B -spin environment, and the probability of finding this configuration (with the geometrical variables r_j, θ_j in the ranges $dr_j, d\theta_j$) is given by

$$\prod_j^N (dV_j/V),$$

where $dV_j = 2\pi r_j^2 dr_j d(\cos\theta_j)$. The problem is to obtain the distribution $I(\Delta\omega)$ of the frequency shifts $\Delta\omega$ for all the A spins in the sample. This is done by integrating over each dV_j , in order to sum over all possible placements of the N B spins, while limiting the summation to those configurations which give frequency shifts in the range $\Delta\omega$ to $\Delta\omega + d(\Delta\omega)$. The constraint is applied by multiplying

$$\prod_j^N (dV_j/V)$$

by

$$d(\Delta\omega) \delta[\Delta\omega - \gamma_A \sum_j \mu_{Bj} (1 - 3 \cos^2\theta_j) / r_j^3],$$

the δ function being written in the integral form

$$(1/2\pi) \int_{-\infty}^{+\infty} d\rho \times \exp[-i\rho \{ \Delta\omega - \gamma_A \sum_j \mu_{Bj} (1 - 3 \cos^2\theta_j) / r_j^3 \}].$$

We thus have

$$\begin{aligned} I(\Delta\omega) d(\Delta\omega) &= d(\Delta\omega) (2\pi)^{-1} \int^V \int^V \cdots \int^V \prod_j \left(\frac{dV_j}{V} \right) \int_{-\infty}^{+\infty} d\rho \\ &\times \exp[-i\rho \{ \Delta\omega - \gamma_A \sum_j \mu_{Bj} (1 - 3 \cos^2\theta_j) / r_j^3 \}]. \quad (\text{A2}) \end{aligned}$$

In the high-temperature limit μ_{Bj} is equally likely to have either of the values $\pm \frac{1}{2} g_B \beta$. This additional random element can conveniently be incorporated into the calculation by allowing r_j to vary from $-\infty$ to $+\infty$ and by writing $2V$ in place of V in order to restore the normalization. We then find that (A2) contains the product of N similar definite integrals. Expanding dV_j , dropping subscripts j and rearranging we have

$$\begin{aligned} I(\Delta\omega) &= (2\pi)^{-1} \int_{-\infty}^{+\infty} d\rho \\ &\times e^{-i\rho \Delta\omega} \left[(2V)^{-1} 2\pi \int_{-\infty}^{+\infty} r^2 dr \int_{-1}^{+1} d(\cos\theta) \right. \\ &\left. \times \exp\{ i(\rho \gamma_A g_B \beta / 2) (1 - 3 \cos^2\theta) / r^3 \} \right]^N. \quad (\text{A3}) \end{aligned}$$

³⁷ No mention is made here of measurements involving electron-nuclear interactions or flip-flop interactions between the electrons. The first can be largely avoided by choosing suitable host materials, and the second by working at fairly high dilutions. Satisfactory theories for these effects of these interactions on the phase memory are not available.

³⁸ H. Margenau, Phys. Rev. **82**, 156 (1951).

³⁹ P. W. Anderson, Phys. Rev. **82**, 342 (1951). The detailed analysis is available only in the form of notes but an equivalent treatment can be found in A. Abragam, *Principles of Nuclear Magnetism* (Oxford University Press, New York, 1961), p. 126. The values for the linewidth given in both these references are $1\frac{1}{2}$ times as large as the value derived in (A9). This arises from the inclusion of a contribution from S_+S_- dipolar terms. We have omitted these terms since we are dealing with unlike spins throughout.

The divergence as $r \rightarrow \infty$, $N \rightarrow \infty$, can be avoided by rewriting (A3) in the form

$$I(\Delta\omega) = (2\pi)^{-1} \int_{-\infty}^{+\infty} d\rho e^{-i\rho\Delta\omega} [1 - V'/V]^N, \quad (\text{A4})$$

where

$$V' = \pi \int_{-\infty}^{+\infty} r^2 dr \int_{-1}^{+1} d(\cos\theta) \times [1 - \exp\{i(\rho\gamma_A g_B \beta/2)(1 - 3\cos^2\theta)/r^3\}]. \quad (\text{A5})$$

In the limit $N \rightarrow \infty$, $V \rightarrow \infty$ we then have

$$I(\Delta\omega) = (2\pi)^{-1} \int_{-\infty}^{+\infty} d\rho \exp(-i\rho\Delta\omega) \exp(-n_B V'), \quad (\text{A6})$$

where $n_B = N/V$ is the number of B spins per cc. Integrating (A5) we have

$$V' = |\rho| (4\pi^2/9\sqrt{3}) \gamma_A g_B \beta. \quad (\text{A7})$$

Therefore,

$$I(\Delta\omega) = \frac{\Delta\omega_{1/2}/\pi}{(\Delta\omega)^2 + (\Delta\omega_{1/2})^2}, \quad (\text{A8})$$

where the half-width

$$\Delta\omega_{1/2} = (4\pi^2/9\sqrt{3}) \gamma_A g_B \beta n_B \simeq 2.53 \gamma_A g_B \beta n_B. \quad (\text{A9})$$

The local field broadening of a resonance line by spins of the same species can be obtained by changing the subscript B to A . This result is $\frac{2}{3}$ of the result normally quoted (see footnote 39), and is applicable when flip-flop processes among the spins are suppressed by static inhomogeneous broadening of the resonance line (i.e., when the experimental linewidth $\gg \Delta\omega_{1/2}$).

Similar calculations can be made for different laws of interaction. It is shown in Ref. 38 that the most significant feature of the interaction is its radial dependence and that this determines the shape of the broadening function. The angular dependence is relatively unimportant and, in most cases, merely introduces a numerical factor into the expression for the linewidth. A departure from randomness in the distribution of B spins about the A spins could, in principle, be taken into account by replacing dV_j by $f(r_j, \theta_j) dV_j$, where $f(r_j, \theta_j) dV_j$ denotes the modified statistical weight for finding a B spin at the coordinates (r, θ) . Assuming separability of the variables in the weighting function we should then have $f(r, \theta) = f'(r)f''(\theta)$, giving in place of (A5) the expression

$$V' = \pi \int_{-\infty}^{+\infty} f'(r) r^2 dr \int_{-1}^{+1} f''(\theta) d(\cos\theta) \times [1 - \exp\{i(\rho\gamma_A g_B \beta/2)(1 - 3\cos^2\theta)/r^3\}]. \quad (\text{A10})$$

By comparing (A5) and (A10) it can be seen that the introduction of $f(r, \theta)$ is equivalent to a change in the law of interaction. It may be verified, for example, by writing $f'(r) = r^{-6/5}$ in (A10) and substituting $r^3 = (r')^5$, that the r^{-3} interaction law in conjunction with an $r^{-6/5}$ clustering function gives the same result as an r^{-5} law with no clustering.

APPENDIX B. THREE-PULSE ECHOES AND THE DIFFUSION KERNEL

In a three-pulse echo sequence let τ denote the time between pulses I and II, and T the time between pulses II and III. The echo, usually termed a stimulated echo, appears at a time τ after pulse III. (Two-pulse echoes generated by the pairs of pulses I-II, I-III, and II-III may also be observed.)⁴⁰ The over-all amplitude decay factor $D(\tau, T)$ for the stimulated echo can be tentatively written as a product $D_\tau(\tau) D_T(\tau, T)$. During the two periods τ , information is stored in the precessing magnetization components M_x, M_y , and the factor $D_\tau(\tau)$ is determined by phase-memory considerations similar to those discussed in the previous section. During the period T the information is stored as a sinusoidal pattern $M_z(\omega_d) \propto \cos(\omega_d \tau + \epsilon)$ in the M_z magnetization spectrum,⁴¹ where ω_d is the difference between the microwave frequency and the Larmor frequency of a given spin packet. The factor $D_T(\tau, T)$ will depend therefore on the rate at which the information contained in the $M_z(\omega_d)$ pattern is erased, either by lattice relaxation of the A spins or as a result of spectral diffusion.

Let us suppose that the broadening of the A -spin line due to the B -spin local field is a small fraction of the total inhomogeneous linewidth. Then the spin packets in the line will each correspond to A spins which have the normal statistical distribution of B -spin environments, and each will show the same diffusion behavior. The diffusion kernel $K(\omega_f - \omega_i, T)$ is defined as the distribution at time T in the ω_d values for those spins which belonged to a spin packet having $\omega_d = \omega_i$ at time zero. Since the initial pattern $M_z(\omega_i) \propto \cos(\omega_i \tau + \epsilon)$, the final distribution $M_z(\omega_f)$ will be proportional to

$$\int \cos(\omega_i \tau + \epsilon) K(\omega_f - \omega_i, T) d\omega_i.$$

Substituting $\omega' = \omega_f - \omega_i$, we have

$$M_z(\omega_f) \propto \cos(\omega_f \tau + \epsilon) \int \cos(\omega' \tau) K(\omega', T) d\omega'. \quad (\text{B1})$$

⁴⁰ If $\gamma H_1 \gg$ the width of the line-shape function $g(\omega)$ then for suitable pulsing conditions (e.g., $\gamma H_1 \tau = 90^\circ, 180^\circ$, and 90° for the three pulses) some of these echoes will be suppressed. If $\gamma H_1 <$ the width of $g(\omega)$, all echoes will usually be visible.

⁴¹ The pattern in $M_z(\omega)$ is not exactly sinusoidal if $\gamma H_1 <$ the width of $g(\omega)$. Numerically computed patterns for particular cases are given by Mims, Nassau, and McGee (Ref. 2, Fig. 2).

The decay factor $D_T(\tau, T)$ is thus the Fourier cosine transform of the diffusion kernel $K(\omega', T)$. [It is assumed above that $K(\omega', T)$ is an even function of ω' . The generalization to odd or to mixed functions $K(\omega', T)$ is trivial and merely involves possible changes in the constant ϵ and hence in the phase of the stimulated echo signal.]

APPENDIX C. FORM OF THE DECAY FUNCTIONS FOR AN r^{-5} INTERACTION LAW

Let us suppose that the energy of interaction between two unlike⁴² ions is $\hbar\omega$ where

$$\omega = k u(\zeta) / r^5, \quad (C1)$$

r is the distance separating the ions, $u(\zeta)$ is a function of the angles defining their orientation relative to one another and to the Zeeman field, and k measures the instantaneous value of the interaction parameter. k could, for example, be the product of two quadrupole moments, of certain additional numerical factors (see Ref. 35), and of a suitable random function denoting the time variation of the interaction. Since the numerical factors for the quadrupole-quadrupole interaction are not easy to calculate or to determine experimentally, we shall absorb them into other numerical constants where possible, and focus attention on the forms of the echo decay functions $E(2\tau)$ and $D_T(\tau, T)$ which result from the r^{-5} interaction law. We follow Ref. 38 in replacing $u(\zeta)$ by a function

$$u(\zeta) = -1 \quad \zeta \leq 0 \\ = +1 \quad \zeta > 0 \quad -1 \leq \zeta \leq 1.$$

The exact form of $u(\zeta)$ is unimportant provided that the mean $\langle \zeta \rangle = 0$. The adoption of alternative forms for $u(\zeta)$ merely changes a numerical constant in the result, but does not alter the form of the decay functions.

The two-pulse echo envelope can be derived according to the Gauss-Markoff model by an argument which follows the same lines as that given in Sec. II. In Eq. (7) $k_j(t') u(\zeta_j) r_j^{-5}$ is substituted for $\gamma_A(\mu_j(t') - \mu_j(0)) \times (1 - 3 \cos^2 \theta_j) r_j^{-3}$. We assume that $k_j(t')$ is a Gaussian random variable, and that

$$\langle k_j(t') k_j(t'') \rangle = \langle (k_j(0))^2 \rangle \exp\{-R_j | t'' - t' | \} \\ = k_0^2 \exp\{-R | t'' - t' | \}.$$

Carrying through the analysis we derive in place of

⁴² The two ions are unlike in the sense that their resonant intervals are separated by an amount which is at least greater than their interaction energy. As in the earlier treatment of the r^{-3} interaction law this could mean that the ions were of the same species, but subject to different strains or other static perturbations.

Eq. (17),

$$V' = 2\pi \int_0^\infty r^2 dr \int d(\xi) \\ \times [1 - \exp[-2B(\tau) k_0^2 \{u(\zeta)\}^2 r^{-10}]]. \quad (C2)$$

Integrating with respect to r , we obtain

$$V' = \frac{1}{3} \{B(\tau)\}^{3/10} k_0^{3/5} \int_0^\infty dx [1 - \exp(-x^{-10/3})] \\ \times \int |u(\zeta)|^{3/5} d\zeta.$$

If the definite integrals are absorbed into k_0 this gives $V' = k_0' \{B(\tau)\}^{3/10}$ in place of (19). The echo envelope $E(2\tau)$ is then $\exp[-n_B k_0' \{B(\tau)\}^{3/10}]$, and in the two limits it reduces to

$$E(2\tau) = \exp[-n_B k_0' R^{0.3} \tau^{0.9}], \quad R\tau \ll 1 \quad (C3a)$$

$$E(2\tau) = \exp[-n_B k_0' R^{-0.3} \tau^{0.3}], \quad R\tau \gg 1. \quad (C3b)$$

In order to calculate $E(2\tau)$ according to the sudden-jump model we need the appropriate diffusion kernel. As in Sec. II this is derived by setting $n_B \rightarrow n_B(1 - e^{-2RT})$, and $\omega \rightarrow \omega_f - \omega_i$ in the line-shape function. In Ref. 38 it is shown that the line-shape function for a $1/r^5$ law of interaction is given by the Fourier transform

$$W(\Delta\omega) = (2\pi)^{-1} \int_{-\infty}^{+\infty} \exp[-n_B k_0'' |\rho|^{3/5}] e^{i\rho\Delta\omega} d\rho \quad (C4)$$

(k_0'' again absorbs the numerical factors arising from the definite integrals with respect to ζ and r). For our purpose it is not necessary to evaluate $W(\Delta\omega)$.⁴³ From (C4), we have the diffusion kernel

$$K(\omega_f - \omega_i, t) = (2\pi)^{-1} \int_{-\infty}^{+\infty} e^{i\rho(\omega_f - \omega_i)} \\ \times \exp[-n_B(1 - e^{-2RT}) k_0'' |\rho|^{3/5}] d\rho. \quad (C5)$$

In the limit of $RT < 1$, (C5) assumes the same form as the general class of functions

$$(2\pi)^{-1} \int \exp[iy(\omega - \omega_0) - t f(y)] dy$$

discussed by Klauder and Anderson [Ref. 1, Eq. (1.11)], for which they show that

$$E(2\tau) = \exp\left\{-2 \int_0^\tau f(t') dt'\right\}.$$

In our particular case $f(y) = 2n_B R k_0'' y^{0.6}$, and thus,

⁴³ The line-shape function $W(\Delta\omega)$ has been computed numerically and is shown in Fig. 1, Ref. 38.

according to the sudden-jump model,

$$E(2\tau) = \exp[-2.5k_0''n_B R\tau^{1.6}]. \quad (C6)$$

It is shown in Appendix B that the three-pulse decay factor $D_T(\tau, T)$ is given by the Fourier transform of the diffusion kernel $K(\omega', T)$. The result for the sudden-jump model can be written down from (C5) as

$$D_T(\tau, T) = \exp[-k_0''n_B(1-e^{-2RT})\tau^{3/5}] \quad (C7a)$$

or

$$D_T(\tau, T) = \exp[-2k_0''n_B RT\tau^{3/5}] \quad \text{if } RT \ll 1. \quad (C7b)$$

The Gauss-Markoff diffusion kernel can be calculated as in Sec. III. In place of Eq. (32) we have

$$\begin{aligned} K(\omega - \omega_0, T) &= (2\pi)^{-1} \int_{-\infty}^{+\infty} d\rho \\ &\times \exp[-i\rho(\omega - \omega_0)] \prod_{j=1}^N \left[V^{-1} \int dV_j \int_{-\infty}^{+\infty} dk_j \right. \\ &\left. \times \exp[i\rho u(\xi_j) r_j^{-5} k_j(T)] f(k_j, T; k_{j0}) \right], \quad (C8a) \end{aligned}$$

where $f(k_j, T; k_{j0})$ is the Gaussian diffusion function (33) which denotes here the distribution of values of k_j at time T . As before we assume that the asymmetric diffusion will average out to zero, provided that the static inhomogeneous broadening is large enough. In place of (34a) and (34b) we obtain

$$K(\omega - \omega_0, T) = (2\pi)^{-1} \int_{-\infty}^{+\infty} \exp[-n_B V'] e^{-i\rho(\omega - \omega_0)} d\rho, \quad (C8b)$$

where

$$\begin{aligned} V' &= 2\pi \int_0^\infty r^2 dr \int d\xi \int_{-\infty}^{+\infty} dk' \\ &\times \{1 - \exp[i\rho u(\xi) r^{-5} k']\} f'(k', T), \quad (C8c) \end{aligned}$$

$f'(k', T)$ being the symmetric diffusion function (34). The integration over r, ξ is the same as that which occurs in the line-shape calculation (Ref. 38), and gives

$$V' = c\rho^{3/5} \int dk' (k')^{3/5} f'(k', T), \quad (C9)$$

where c contains the values of definite integrals and other numerical constants. Substituting $f'(k', T)$ and integrating we have

$$V' = c'\rho^{3/5} (1 - e^{-2RT})^{3/10}. \quad (C10)$$

Combining (C8b) and (C10) we derive the diffusion kernel as a Fourier integral

$$\begin{aligned} K(\omega - \omega_0, T) &= (2\pi)^{-1} \\ &\times \int_{-\infty}^{+\infty} \exp[-n_B c' |\rho|^{3/5} (1 - e^{-2RT})^{3/10}] e^{-i\rho(\omega - \omega_0)} d\rho. \quad (C11) \end{aligned}$$

$K(\omega - \omega_0, T)$ can be made to coincide with the line-shape function (C4) in the limit $RT \rightarrow \infty$ by equating c' and k_0'' . There is no need to evaluate (C11) since the three-pulse decay factor $D_T(\tau, T)$ is the Fourier transform of the diffusion kernel (Appendix B). Thus

$$D_T(\tau, T) = \exp[-n_B k_0'' \tau^{3/5} (1 - e^{-2RT})^{3/10}] \quad (C12a)$$

or

$$D_T(\tau, T) = \exp[-2^{3/10} k_0'' R^{3/10} \tau^{3/5} T^{3/10}] \quad \text{if } RT \ll 1. \quad (C12b)$$

It was pointed out at the end of Appendix A that clustering of the ions will produce effects on $E(2\tau)$ and $D_T(\tau, T)$ which are equivalent to the effects produced by a change in the law of interaction. In the above case the results are equivalent to those which would be obtained by retaining the r^{-3} interaction law while introducing a weighting function $f(r) = r^{-6/5}$ to denote the enhanced probability of finding a B spin at the distance r from an A spin.